

We are IntechOpen, the world's leading publisher of Open Access books Built by scientists, for scientists

6,900

Open access books available

186,000

International authors and editors

200M

Downloads

Our authors are among the

154

Countries delivered to

TOP 1%

most cited scientists

12.2%

Contributors from top 500 universities



WEB OF SCIENCE™

Selection of our books indexed in the Book Citation Index
in Web of Science™ Core Collection (BKCI)

Interested in publishing with us?
Contact book.department@intechopen.com

Numbers displayed above are based on latest data collected.
For more information visit www.intechopen.com



The Effect of Weak Fields at Multiple Frequencies on the Scattering and Generation of Waves by Nonlinear Layered Media

Lutz Angermann and Vasyl V. Yatsyk

Additional information is available at the end of the chapter

<http://dx.doi.org/10.5772/50679>

1. Introduction

The chapter deals with the effects of weak fields at multiple frequencies on the scattering and generation of waves by an isotropic, nonmagnetic, linearly polarised (E-polarisation), layered, cubically polarisable, dielectric structure. In the domain of resonance frequencies we consider wave packets consisting of both strong electromagnetic fields at the excitation frequency of the nonlinear structure, leading to the generation of waves, and of weak fields at the multiple frequencies, which do not lead to the generation of harmonics but influence on the process of scattering and generation of waves by the nonlinear structure. The electromagnetic waves for a nonlinear layer with a cubic polarisability of the medium can be described by an infinite system of nonlinear boundary-value problems in the frequency domain. As has been shown in previous articles of the authors ([3], [4]), in the study of particular nonlinear effects it is possible to restrict this system to a finite number of equations. If the classical formulation of the problem is supplemented by the condition of phase synchronism, we arrive at a self-consistent formulation of a system of boundary-value problems with respect to the components of the scattered and generated fields. It is known that this system is equivalent to a system of nonlinear boundary-value problems of Sturm-Liouville type and also to a system of one-dimensional nonlinear Fredholm integral equations of the second kind.

The solution of the system of integral equations is approximated by the help of numerical algorithms. Those include the application of suitable quadrature rules and iterative procedures to solve the resulting nonlinear algebraic problems. Since in each iteration step the solution of linear algebraic systems is required, the approximate solution of the nonlinear problems is described by means of solutions of linear problems with an induced nonlinear permittivity.

In continuation of our results from previous works ([3], [4]), where we only considered one excitation field at the basic frequency, here results of calculations of characteristics of the

scattered and generated fields of plane waves are presented, taking into account the influence of weak fields at multiple frequencies on the cubically polarisable layer. We restrict ourselves to the investigation of the third harmonic generated by layers with a positive value of the cubic susceptibility of the medium.

Within the framework of the self-consistent system which is given by a system of nonlinear integral equations, we show the following. The variation of the imaginary parts of the permittivities of the layer at the multiple frequencies can take both positive and negative values along the height of the nonlinear layer. It is induced by the nonlinear part of the permittivities and is caused by the loss of energy in the nonlinear medium which is spent for the generation of the electromagnetic fields. The magnitudes of these variations are determined by the amplitude and phase characteristics of the fields which are scattered and generated by the nonlinear layer.

Layers with negative and positive values of the coefficient of cubic susceptibility of the nonlinear medium have fundamentally different scattering and generation properties. In the case of negative values of the susceptibility, a decanalisation of the electromagnetic field can be detected. The maximal portion of the total energy generated in the third harmonic is observed in the direction normal to the structure and nearly amounts to 4% of the total dissipated energy. For a layer with a positive value of the susceptibility an effect of energy canalisation is observed (see [4]). Increasing intensities of the incidents fields lead to an increase of the angle of transparency which increasingly deviates from the direction normal to the layer. In this case, the maximal portion of energy generated in the third harmonic is observed near the angle of transparency of the nonlinear layer. In the numerical experiments there have been reached intensities of the excitation field of the layer such that the relative portion of the total energy generated in the third harmonic is about 35% (see [4]).

In the chapter the effect of weak fields at multiple frequencies on the scattering and generation of waves is investigated numerically. The results indicate a possibility of designing a frequency multiplier and nonlinear dielectrics with controllable permittivity.

2. The mathematical model

We consider a layered nonlinear medium which is located in an infinite plate of thickness $4\pi\delta$, where $\delta > 0$ is a given parameter: $\{\mathbf{r} = (x, y, z)^\top \in \mathbb{R}^3 : |z| \leq 2\pi\delta\}$.

It is assumed that the vector of the polarisation moment \mathbf{P} can be expanded in terms of the electric field intensity \mathbf{E} as follows:

$$\mathbf{P} = \chi^{(1)}\mathbf{E} + (\chi^{(2)}\mathbf{E})\mathbf{E} + ((\chi^{(3)}\mathbf{E})\mathbf{E})\mathbf{E} + \dots, \quad (1)$$

where $\chi^{(1)}$, $\chi^{(2)}$, $\chi^{(3)}$ are the media susceptibility tensors of rank two, three and four, with components $\{\chi_{ij}^{(1)}\}_{i,j=1}^3$, $\{\chi_{ijk}^{(2)}\}_{i,j,k=1}^3$ and $\{\chi_{ijkl}^{(3)}\}_{i,j,k,l=1}^3$, respectively (see [5]). In the case of isotropic media, the quadratic term disappears.

It is convenient to split \mathbf{P} into its linear and nonlinear parts as $\mathbf{P} = \mathbf{P}^{(L)} + \mathbf{P}^{(NL)} := \chi^{(1)}\mathbf{E} + \mathbf{P}^{(NL)}$. Similarly, with $\epsilon := \mathbf{I} + 4\pi\chi^{(1)}$ and $\mathbf{D}^{(L)} := \epsilon\mathbf{E}$, where \mathbf{I} denotes the identity in \mathbb{C}^3 ,

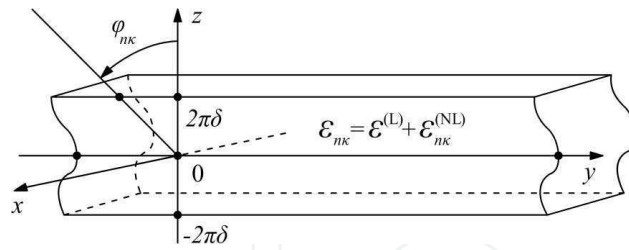


Figure 1. The nonlinear dielectric layered structure

the displacement field \mathbf{D} can be decomposed as

$$\mathbf{D} = \mathbf{D}^{(L)} + 4\pi\mathbf{P}^{(NL)}. \quad (2)$$

ϵ is the linear term of the permittivity tensor. Furthermore, if the media under consideration are nonmagnetic, isotropic and transversely inhomogeneous w.r.t. z , i.e. $\epsilon = \epsilon^{(L)}\mathbf{I}$ with a scalar, possibly complex-valued function $\epsilon^{(L)} = \epsilon^{(L)}(z)$, if the wave is linearly E-polarised, i.e.

$$\mathbf{E} = (E_1, 0, 0)^\top, \quad \mathbf{H} = (0, H_2, H_3)^\top, \quad (3)$$

and if the electric field \mathbf{E} is homogeneous w.r.t. the coordinate x , i.e. $\mathbf{E}(\mathbf{r}, t) = (E_1(t; y, z), 0, 0)^\top$, then the Maxwell's equations together with (2) are simplified to

$$\nabla^2 \mathbf{E} - \frac{\epsilon^{(L)}}{c^2} \frac{\partial^2}{\partial t^2} \mathbf{E} - \frac{4\pi}{c^2} \frac{\partial^2}{\partial t^2} \mathbf{P}^{(NL)} = 0, \quad (4)$$

where ∇^2 reduces to the Laplacian w.r.t. y and z , i.e. $\nabla^2 := \partial^2/\partial y^2 + \partial^2/\partial z^2$.

A stationary electromagnetic wave (with the oscillation frequency $\omega > 0$) propagating in a nonlinear dielectric structure gives rise to a field containing all frequency harmonics (see [20], [22], and other authors). Therefore, representing \mathbf{E} , $\mathbf{P}^{(NL)}$ via Fourier series

$$\mathbf{E}(\mathbf{r}, t) = \frac{1}{2} \sum_{s \in \mathbb{Z}} \mathbf{E}(\mathbf{r}, s\omega) e^{-is\omega t}, \quad \mathbf{P}^{(NL)}(\mathbf{r}, t) = \frac{1}{2} \sum_{s \in \mathbb{Z}} \mathbf{P}^{(NL)}(\mathbf{r}, s\omega) e^{-is\omega t}, \quad (5)$$

we obtain from (4) an infinite system of coupled equations w.r.t. the Fourier amplitudes. In the case of a three-component E-polarised electromagnetic field (3), this system reduces to a system of scalar equations w.r.t. E_1 :

$$\Delta E_1(\mathbf{r}, s\omega) + \frac{\epsilon^{(L)}(s\omega)^2}{c^2} E_1(\mathbf{r}, s\omega) + \frac{4\pi(s\omega)^2}{c^2} P_1^{(NL)}(\mathbf{r}, s\omega) = 0, \quad s \in \mathbb{N}. \quad (6)$$

In writing equation (6), the property $E_1(\mathbf{r}; j\omega) = \bar{E}_1(\mathbf{r}; -j\omega)$ of the Fourier coefficients and the lack of influence of the static electric field $E_1(\mathbf{r}, s\omega)|_{s=0} = 0$ on the nonlinear structure were taken into consideration.

We assume that the main contribution to the nonlinearity is introduced by the term $\mathbf{P}^{(NL)}(\mathbf{r}, s\omega)$ (cf. [25], [14], [8], [1], [24], [10], [19], [11]), and we take only the lowest-order terms in the Taylor series expansion of the nonlinear part $\mathbf{P}^{(NL)}(\mathbf{r}, s\omega) = \left(P_1^{(NL)}(\mathbf{r}, s\omega), 0, 0\right)^\top$ of the polarisation vector in the vicinity of the zero value of the electric field intensity, cf. (1). In this case, the only nontrivial component of the polarisation vector is determined by susceptibility tensor of the third order $\chi^{(3)}$. In the time domain, this component can be represented in the form (cf. (1) and (5)):

$$P_1^{(NL)}(\mathbf{r}, t) \doteq \frac{1}{8} \sum_{\substack{n,m,p,s \in \mathbb{Z} \setminus \{0\} \\ n+m+p=s}} \chi_{1111}^{(3)}(s\omega; n\omega, m\omega, p\omega) E_1(\mathbf{r}, n\omega) E_1(\mathbf{r}, m\omega) E_1(\mathbf{r}, p\omega) e^{-is\omega t}, \quad (7)$$

where the symbol \doteq means that higher-order terms are neglected. Applying to (7) the Fourier transform w.r.t. time, we obtain an expansion in the frequency domain:

$$P_1^{(NL)}(\mathbf{r}, s\omega) = \frac{1}{4} \sum_{j \in \mathbb{N}} 3\chi_{1111}^{(3)}(s\omega; j\omega, -j\omega, s\omega) |E_1(\mathbf{r}, j\omega)|^2 E_1(\mathbf{r}, s\omega) + \frac{1}{4} \sum_{\substack{n,m,p \in \mathbb{Z} \setminus \{0\} \\ n \neq -m, p=s \\ m \neq -p, n=s \\ n \neq -p, m=s \\ n+m+p=s}} \chi_{1111}^{(3)}(s\omega; n\omega, m\omega, p\omega) E_1(\mathbf{r}, n\omega) E_1(\mathbf{r}, m\omega) E_1(\mathbf{r}, p\omega). \quad (8)$$

We see that, under the above assumptions, the electromagnetic waves in a nonlinear medium with a cubic polarisability are described by an infinite system (6) and (8) of coupled nonlinear equations ([25], [14], [8], [2]).

Here we study nonlinear effects involving the waves at the first three frequency components of E_1 only. That is, we further neglect the influence of harmonics of order higher than 3. Then it is possible to restrict the examination of the system (6) and (8) to three equations, and also to leave particular terms in the representation of the polarisation coefficients. Taking into account only the nontrivial terms in the expansion of the polarisation coefficients and using the so-called *Kleinman's rule* (i.e. the equality of all the coefficients $\chi_{1111}^{(3)}$ at the multiple frequencies, [7], [9]), we arrive at the following system:

$$\begin{aligned} & \Delta E_1(\mathbf{r}, n\kappa) + (n\kappa)^2 \varepsilon_{n\kappa}(z, \alpha(z), E_1(\mathbf{r}, \kappa), E_1(\mathbf{r}, 2\kappa), E_1(\mathbf{r}, 3\kappa)) \\ & = -\delta_{n1} \kappa^2 \alpha(z) E_1^2(\mathbf{r}, 2\kappa) \bar{E}_1(\mathbf{r}, 3\kappa) \\ & \quad - \delta_{n3} (3\kappa)^2 \alpha(z) \left\{ \frac{1}{3} E_1^3(\mathbf{r}, \kappa) + E_1^2(\mathbf{r}, 2\kappa) \bar{E}_1(\mathbf{r}, \kappa) \right\}, \quad n = 1, 2, 3, \end{aligned} \quad (9)$$

with $\kappa := \frac{\omega}{c} = \frac{2\pi}{\lambda}$, $\varepsilon_{n\kappa} := \begin{cases} 1, & |z| > 2\pi\delta, \\ \varepsilon^{(L)} + \varepsilon_{n\kappa}^{(NL)}, & |z| \leq 2\pi\delta, \end{cases}$ and $\varepsilon^{(L)} := 1 + 4\pi\chi_{11}^{(1)}$,

$$\begin{aligned} \varepsilon_{n\kappa}^{(NL)} = & \alpha(z) [|E_1(\mathbf{r}, \kappa)|^2 + |E_1(\mathbf{r}, 2\kappa)|^2 + |E_1(\mathbf{r}, 3\kappa)|^2 \\ & + \delta_{n1} \frac{[\overline{E_1(\mathbf{r}, \kappa)}]^2}{E_1(\mathbf{r}, \kappa)} E_1(\mathbf{r}, 3\kappa) + \delta_{n2} \frac{\overline{E_1(\mathbf{r}, 2\kappa)}}{E_1(\mathbf{r}, 2\kappa)} E_1(\mathbf{r}, \kappa) E_1(\mathbf{r}, 3\kappa)], \end{aligned} \tag{10}$$

where $\alpha(z) := 3\pi\chi_{1111}^{(3)}(z)$ is the so-called *function of cubic susceptibility* and δ_{nj} denotes Kronecker's symbol. For transversely inhomogeneous media (a layer or a layered structure), the linear part $\varepsilon^{(L)}$ of the permittivity is described by a piecewise smooth or even a piecewise constant function. Similarly, the function of the cubic susceptibility $\alpha = \alpha(z)$ is also a piecewise smooth or even a piecewise constant function. This assumption allows us to investigate the scattering and generation characteristics of a nonlinear layer and of a layered structure (consisting of a finite number of linear and nonlinear dielectric layers) within one and the same mathematical model.

Here and in what follows we use the following notation: (\mathbf{r}, t) are dimensionless spatial-temporal coordinates such that the thickness of the layer is equal to $4\pi\delta$. The time-dependence is determined by the factors $\exp(-in\omega t)$, where $\omega = \kappa c$ is the dimensionless circular frequency and κ is a dimensionless frequency parameter. This parameter characterises the ratio of the true thickness h of the layer to the free-space wavelength λ , i.e. $h/\lambda = 2\kappa\delta$. $c = (\varepsilon_0\mu_0)^{-1/2}$ denotes a dimensionless parameter, equal to the absolute value of the speed of light in the medium containing the layer ($\Im m c = 0$). ε_0 and μ_0 are the material parameters of the medium. The absolute values of the true variables \mathbf{r}', t', ω' are given by the formulas $\mathbf{r}' = h\mathbf{r}/4\pi\delta$, $t' = th/4\pi\delta$, $\omega' = \omega 4\pi\delta/h$.

The scattered and generated field in a transversely inhomogeneous, nonlinear dielectric layer excited by a plane wave is *quasi-homogeneous* along the coordinate y , hence it can be represented as

$$(C1) \quad E_1(\mathbf{r}, n\kappa) =: E_1(n\kappa; y, z) := U(n\kappa; z) \exp(i\phi_{n\kappa}y), \quad n = 1, 2, 3.$$

Here $U(n\kappa; z)$ and $\phi_{n\kappa} := n\kappa \sin \varphi_{n\kappa}$ denote the complex-valued transverse component of the Fourier amplitude of the electric field and the value of the longitudinal propagation constant (longitudinal wave-number) at the frequency $n\kappa$, respectively, where $\varphi_{n\kappa}$ is the given angle of incidence of the exciting field of frequency $n\kappa$ (cf. Fig. 1).

Furthermore we require that the following *condition of the phase synchronism of waves* is satisfied:

$$(C2) \quad \phi_{n\kappa} = n\phi_{\kappa}, \quad n = 1, 2, 3.$$

Then the permittivity of the nonlinear layer can be expressed as

$$\begin{aligned} \varepsilon_{n\kappa}(z, \alpha(z), E_1(\mathbf{r}, \kappa), E_1(\mathbf{r}, 2\kappa), E_1(\mathbf{r}, 3\kappa)) = & \varepsilon_{n\kappa}(z, \alpha(z), U(\kappa; z), U(2\kappa; z), U(3\kappa; z)) \\ = & \varepsilon^{(L)}(z) + \alpha(z) [|U(\kappa; z)|^2 + |U(2\kappa; z)|^2 + |U(3\kappa; z)|^2 \\ & + \delta_{n1} |U(\kappa; z)| |U(3\kappa; z)| \exp\{i[-3\arg(U(\kappa; z)) + \arg(U(3\kappa; z))]\} \\ & + \delta_{n2} |U(\kappa; z)| |U(3\kappa; z)| \exp\{i[-2\arg(U(2\kappa; z)) + \arg(U(\kappa; z)) + \arg(U(3\kappa; z))]\}], \end{aligned} \tag{11}$$

$n = 1, 2, 3.$

A more detailed explanation of the condition (C2) can be found in [3, Sect. 3]. In the considered case of spatially quasi-homogeneous (along the coordinate y) electromagnetic fields (C1), the condition of the phase synchronism of waves (C2) reads as

$$\sin \varphi_{n\kappa} = \sin \varphi_{\kappa}, \quad n = 1, 2, 3.$$

Consequently, the given angle of incidence of a plane wave at the frequency κ coincides with the possible directions of the angles of incidence of plane waves at the multiple frequencies $n\kappa$, i.e. $\varphi_{n\kappa} = \varphi_{\kappa}$, $n = 1, 2, 3$. The angles of the wave scattered by the layer are equal to $\varphi_{n\kappa}^{\text{scat}} = -\varphi_{n\kappa}$ in the zone of reflection $z > 2\pi\delta$ and $\varphi_{n\kappa}^{\text{scat}} = \pi + \varphi_{n\kappa}$ and in the zone of transmission of the nonlinear layer $z < -2\pi\delta$, where all angles are measured counter-clockwise in the (y, z) -plane from the z -axis (cf. Fig. 1).

The conditions (C1), (C2) allow a further simplification of the system (9). Before we do so, we want to make a few comments on specific cases which have already been discussed in the literature. First we mention that the effect of a weak quasi-homogeneous electromagnetic field (C1) on the nonlinear dielectric structure such that harmonics at multiple frequencies are not generated, i.e. $E_1(\mathbf{r}, 2\kappa) = 0$ and $E_1(\mathbf{r}, 3\kappa) = 0$, reduces to find the electric field component $E_1(\mathbf{r}, \kappa)$ determined by the first equation of the system (9). In this case, a diffraction problem for a plane wave on a nonlinear dielectric layer with a Kerr-type nonlinearity $\varepsilon_{n\kappa} = \varepsilon^{(L)}(z) + \alpha(z)|E_1(\mathbf{r}, \kappa)|^2$ and a vanishing right-hand side is to be solved, see [1, 8, 11, 14, 19, 24, 25]. The generation process of a field at the triple frequency 3κ by the nonlinear dielectric structure is caused by a strong incident electromagnetic field at the frequency κ and can be described by the first and third equations of the system (9) only, i.e. $n = 1, 3$. Since the right-hand side of the second equation in (9) is equal to zero, we may set $E_1(\mathbf{r}, 2\kappa) = 0$ corresponding to the homogeneous boundary condition w.r.t. $E_1(\mathbf{r}, 2\kappa)$. Therefore the second equation in (9) can be completely omitted, see [2] and the numerical results in [3], [4].

A further interesting problem consists in the investigation of the influence of a packet of waves on the generation of the third harmonic, if a strong incident field at the basic frequency κ and, in addition, weak incident quasi-homogeneous electromagnetic fields at the double and triple frequencies $2\kappa, 3\kappa$ (which alone do not generate harmonics at multiple frequencies) excite the nonlinear structure. Then we have to take into account all three equations of system (9). This is caused by the inhomogeneity of the corresponding problem, where a weak incident field at the double frequency 2κ (or two weak fields at the frequencies 2κ and 3κ) excites (resp. excite) the dielectric medium.

So we consider the problem of scattering and generation of waves on a nonlinear, layered, cubically polarisable structure, which is excited by a packet of plane waves consisting of a strong field at the frequency κ (which generates a field at the triple frequency 3κ) and of weak fields at the frequencies 2κ and 3κ (having an impact on the process of third harmonic generation due to the contribution of weak electromagnetic fields)

$$\left\{ E_1^{\text{inc}}(\mathbf{r}, n\kappa) := E_1^{\text{inc}}(n\kappa; y, z) := a_{n\kappa}^{\text{inc}} \exp\left(i(\varphi_{n\kappa} y - \Gamma_{n\kappa}(z - 2\pi\delta))\right) \right\}_{n=1}^3, \quad z > 2\pi\delta, \quad (12)$$

with amplitudes $a_{n\kappa}^{\text{inc}}$ and angles of incidence $\varphi_{n\kappa}$, $|\varphi| < \pi/2$ (cf. Fig. 1), where $\phi_{n\kappa} := n\kappa \sin \varphi_{n\kappa}$ are the longitudinal propagation constants (longitudinal wave-numbers) and $\Gamma_{n\kappa} := \sqrt{(n\kappa)^2 - \phi_{n\kappa}^2}$ are the transverse propagation constants (transverse wave-numbers).

In this setting, if a packet of plane waves excites a nonmagnetic, isotropic, linearly polarised (i.e.

$$\mathbf{E}(\mathbf{r}, n\kappa) = (E_1(n\kappa; y, z), 0, 0)^\top, \quad \mathbf{H}(\mathbf{r}, n\kappa) = \left(0, \frac{1}{i n \omega \mu_0} \frac{\partial E_1(n\kappa; y, z)}{\partial z}, -\frac{1}{i n \omega \mu_0} \frac{\partial E_1(n\kappa; y, z)}{\partial y} \right)^\top$$

(E-polarisation)), transversely inhomogeneous $\varepsilon^{(L)} = \varepsilon^{(L)}(z) = 1 + 4\pi\chi_{11}^{(1)}(z)$ dielectric layer (see Fig. 1) with a cubic polarisability $\mathbf{P}^{(NL)}(\mathbf{r}, n\kappa) = (P_1^{(NL)}(n\kappa; y, z), 0, 0)^\top$ of the medium, the complex amplitudes of the total fields

$$E_1(\mathbf{r}, n\kappa) := E_1(n\kappa; y, z) := U(n\kappa; z) \exp(i\phi_{n\kappa}y) := E_1^{\text{inc}}(n\kappa; y, z) + E_1^{\text{scat}}(n\kappa; y, z)$$

satisfy the system of equations (cf. (9) – (10))

$$\begin{cases} \nabla^2 E_1(\mathbf{r}, \kappa) + \kappa^2 \varepsilon_\kappa(z, \alpha(z), E_1(\mathbf{r}, \kappa), E_1(\mathbf{r}, 2\kappa), E_1(\mathbf{r}, 3\kappa)) E_1(\mathbf{r}, \kappa) \\ \quad = -\alpha(z) \kappa^2 E_1^2(\mathbf{r}, 2\kappa) \bar{E}_1(\mathbf{r}, 3\kappa), \\ \nabla^2 E_1(\mathbf{r}, 2\kappa) + (2\kappa)^2 \varepsilon_{2\kappa}(z, \alpha(z), E_1(\mathbf{r}, \kappa), E_1(\mathbf{r}, 2\kappa), E_1(\mathbf{r}, 3\kappa)) E_1(\mathbf{r}, 2\kappa) = 0, \\ \nabla^2 E_1(\mathbf{r}, 3\kappa) + (3\kappa)^2 \varepsilon_{3\kappa}(z, \alpha(z), E_1(\mathbf{r}, \kappa), E_1(\mathbf{r}, 2\kappa), E_1(\mathbf{r}, 3\kappa)) E_1(\mathbf{r}, 3\kappa) \\ \quad = -\alpha(z) (3\kappa)^2 \left\{ \frac{1}{3} E_1^3(\mathbf{r}, \kappa) + E_1^2(\mathbf{r}, 2\kappa) \bar{E}_1(\mathbf{r}, \kappa) \right\} \end{cases} \quad (13)$$

together with the following conditions, where $\mathbf{E}_{\text{tg}}(n\kappa; y, z)$ and $\mathbf{H}_{\text{tg}}(n\kappa; y, z)$ denote the tangential components of the intensity vectors of the full electromagnetic field $\{\mathbf{E}(n\kappa; y, z)\}_{n=1,2,3}$, $\{\mathbf{H}(n\kappa; y, z)\}_{n=1,2,3}$:

- (C1) $E_1(n\kappa; y, z) = U(n\kappa; z) \exp(i\phi_{n\kappa}y)$, $n = 1, 2, 3$
 (the quasi-homogeneity condition w.r.t. the spatial variable y introduced above),
- (C2) $\phi_{n\kappa} = n\phi_\kappa$, $n = 1, 2, 3$,
 (the condition of phase synchronism of waves introduced above),
- (C3) $\mathbf{E}_{\text{tg}}(n\kappa; y, z)$ and $\mathbf{H}_{\text{tg}}(n\kappa; y, z)$ (i.e. $E_1(n\kappa; y, z)$ and $H_2(n\kappa; y, z)$)
 are continuous at the boundary layers of the nonlinear structure,
- (C4) $E_1^{\text{scat}}(n\kappa; y, z) = \begin{Bmatrix} a_{n\kappa}^{\text{scat}} \\ b_{n\kappa}^{\text{scat}} \end{Bmatrix} \exp(i(\phi_{n\kappa}y \pm \Gamma_{n\kappa}(z \mp 2\pi\delta)))$, $z \gtrless \pm 2\pi\delta$, $n = 1, 2, 3$
 (the radiation condition w.r.t. the scattered and generated fields).

The condition (C4) provides a physically consistent behaviour of the energy characteristics of scattering and generation. It guarantees the absence of waves coming from infinity (i.e.

$z = \pm\infty$), see [12]. We study the scattering and generation properties of the nonlinear layer, where in (C4) we always have

$$\Im \Gamma_{n\kappa} = 0, \quad \Re \Gamma_{n\kappa} > 0. \quad (14)$$

Note that (C4) is also applicable for the analysis of the wave-guide properties of the layer, where $\Im \Gamma_{n\kappa} > 0$, $\Re \Gamma_{n\kappa} = 0$. The desired solution of the scattering and generation problem (13) under the conditions (C1) – (C4) can be represented as follows:

$$E_1(n\kappa; y, z) = U(n\kappa; z) \exp(i\phi_{n\kappa} y) \\ = \begin{cases} a_{n\kappa}^{\text{inc}} \exp(i(\phi_{n\kappa} y - \Gamma_{n\kappa}(z - 2\pi\delta))) + a_{n\kappa}^{\text{scat}} \exp(i(\phi_{n\kappa} y + \Gamma_{n\kappa}(z - 2\pi\delta))), & z > 2\pi\delta, \\ U(n\kappa; z) \exp(i\phi_{n\kappa} y), & |z| \leq 2\pi\delta, \\ b_{n\kappa}^{\text{scat}} \exp(i(\phi_{n\kappa} y - \Gamma_{n\kappa}(z + 2\pi\delta))), & z < -2\pi\delta, \end{cases} \quad (15) \\ n = 1, 2, 3.$$

Substituting this representation into the system (13), the following system of nonlinear ordinary differential equations results, where “'” denotes the differentiation w.r.t. z :

$$U''(n\kappa; z) + \{ \Gamma_{n\kappa}^2 - (n\kappa)^2 [1 - \varepsilon_{n\kappa}(z, \alpha(z), U(\kappa; z), U(2\kappa; z), U(3\kappa; z))] \} U(n\kappa; z) \\ = -(n\kappa)^2 \alpha(z) \left(\delta_{n1} U^2(2\kappa; z) \bar{U}(3\kappa; z) + \delta_{n3} \left\{ \frac{1}{3} U^3(\kappa; z) + U^2(2\kappa; z) \bar{U}(\kappa; z) \right\} \right), \quad (16) \\ |z| \leq 2\pi\delta, \quad n = 1, 2, 3.$$

The boundary conditions follow from the continuity of the tangential components of the full fields of scattering and generation $\{ \mathbf{E}_{\text{tg}}(n\kappa; y, z) \}_{n=1,2,3}$, $\{ \mathbf{H}_{\text{tg}}(n\kappa; y, z) \}_{n=1,2,3}$ at the boundaries $z = \pm 2\pi\delta$ of the nonlinear layer (cf. (C3)). According to (C3) and the representation of the electrical components of the electromagnetic field (15), at the boundary of the nonlinear layer we obtain:

$$U(n\kappa; 2\pi\delta) = a_{n\kappa}^{\text{scat}} + a_{n\kappa}^{\text{inc}}, \quad U'(n\kappa; 2\pi\delta) = i\Gamma_{n\kappa} (a_{n\kappa}^{\text{scat}} - a_{n\kappa}^{\text{inc}}), \\ U(n\kappa; -2\pi\delta) = b_{n\kappa}^{\text{scat}}, \quad U'(n\kappa; -2\pi\delta) = -i\Gamma_{n\kappa} b_{n\kappa}^{\text{scat}}, \quad n = 1, 2, 3. \quad (17)$$

Eliminating in (17) the unknown values of the complex amplitudes $\{ a_{n\kappa}^{\text{scat}} \}_{n=1,2,3}$, $\{ b_{n\kappa}^{\text{scat}} \}_{n=1,2,3}$ of the scattered and generated fields and taking into consideration that $a_{n\kappa}^{\text{inc}} = U^{\text{inc}}(n\kappa; 2\pi\delta)$, we arrive at the desired boundary conditions for the problem (16):

$$i\Gamma_{n\kappa} U(n\kappa; -2\pi\delta) + U'(n\kappa; -2\pi\delta) = 0, \\ i\Gamma_{n\kappa} U(n\kappa; 2\pi\delta) - U'(n\kappa; 2\pi\delta) = 2i\Gamma_{n\kappa} a_{n\kappa}^{\text{inc}}, \quad n = 1, 2, 3. \quad (18)$$

The system of ordinary differential equations (16) and the boundary conditions (18) form a semi-linear boundary-value problem of Sturm-Liouville type, see also [2, 14, 15, 25]. The existence and uniqueness of a weak solution of the nonlinear boundary-value problem (16) and (18) have been demonstrated in [4, Sect. 4].

The problem (13), (C1) – (C4) can also be reduced to finding solutions of one-dimensional nonlinear integral equations w.r.t. the components $U(n\kappa; z)$, $n = 1, 2, 3$, $z \in [-2\pi\delta, 2\pi\delta]$, of the fields scattered and generated in the nonlinear layer (cf. [3], [2], [15], [25], [14], [8]):

$$\begin{aligned}
 & U(n\kappa; z) + \frac{i(n\kappa)^2}{2\Gamma_{n\kappa}} \int_{-2\pi\delta}^{2\pi\delta} \exp(i\Gamma_{n\kappa}|z - z_0|) \times \\
 & \quad \times [1 - \varepsilon_{n\kappa}(z_0, \alpha(z_0), U(\kappa; z_0), U(2\kappa; z_0), U(3\kappa; z_0))] U(n\kappa; z_0) dz_0 \\
 = & \delta_{n1} \frac{i(n\kappa)^2}{2\Gamma_{n\kappa}} \int_{-2\pi\delta}^{2\pi\delta} \exp(i\Gamma_{n\kappa}|z - z_0|) \alpha(z_0) U^2(2\kappa; z_0) \bar{U}(3\kappa; z_0) dz_0 \\
 & + \delta_{n3} \frac{i(n\kappa)^2}{2\Gamma_{n\kappa}} \int_{-2\pi\delta}^{2\pi\delta} \exp(i\Gamma_{n\kappa}|z - z_0|) \alpha(z_0) \left\{ \frac{1}{3} U^3(\kappa; z_0) + U^2(2\kappa; z_0) \bar{U}(\kappa; z_0) \right\} dz_0 \\
 & + U^{\text{inc}}(n\kappa; z), \quad |z| \leq 2\pi\delta, \quad n = 1, 2, 3.
 \end{aligned} \tag{19}$$

Here $U^{\text{inc}}(n\kappa; z) = a_{n\kappa}^{\text{inc}} \exp[-i\Gamma_{n\kappa}(z - 2\pi\delta)]$, $n = 1, 2, 3$.

The solution of the original problem (13), (C1) – (C4), represented as (15), can be obtained from (19) using the formulas

$$U(n\kappa; 2\pi\delta) = a_{n\kappa}^{\text{inc}} + a_{n\kappa}^{\text{scat}}, \quad U(n\kappa; -2\pi\delta) = b_{n\kappa}^{\text{scat}}, \quad n = 1, 2, 3, \tag{20}$$

(cf. (C3)). The system (19) can be regarded as an integral representation of the desired solution of (13), (C1) – (C4) (i.e. solutions of the form $E_1(n\kappa; y, z) = U(n\kappa; z) \exp(i\phi_{n\kappa}y)$, $n = 1, 2, 3$, see (15)) for points located outside the nonlinear layer: $\{(y, z) : |y| < \infty, |z| > 2\pi\delta\}$. Indeed, given the solution of nonlinear integral equations (19) in the region $|z| \leq 2\pi\delta$, the substitution into the integrals of (19) leads to explicit expressions of the desired solutions $U(n\kappa; z)$ for points $|z| > 2\pi\delta$ outside the nonlinear layer at each frequency $n\kappa$, $n = 1, 2, 3$.

In the case of a linear system (19), i.e. if $\alpha \equiv 0$, the problem of existence and uniqueness of solutions has been investigated in [16], [12]. Sufficient conditions for the existence and uniqueness of solutions $U(n\kappa; \cdot) \in L_2(-2\pi\delta, 2\pi\delta)$ to the nonlinear system (19) have been given in [4, Sect. 6].

3. A self-consistent approach to the numerical analysis of the nonlinear integral equations

According to [3], [2], the application of suitable quadrature rules to the system of nonlinear integral equations (19) leads to a system of complex-valued nonlinear algebraic equations of the second kind:

$$\begin{cases}
 (\mathbf{I} - \mathbf{B}_\kappa(\mathbf{U}_\kappa, \mathbf{U}_{2\kappa}, \mathbf{U}_{3\kappa})) \mathbf{U}_\kappa = \mathbf{C}_\kappa(\mathbf{U}_{2\kappa}, \mathbf{U}_{3\kappa}) + \mathbf{U}_\kappa^{\text{inc}}, \\
 (\mathbf{I} - \mathbf{B}_{2\kappa}(\mathbf{U}_\kappa, \mathbf{U}_{2\kappa}, \mathbf{U}_{3\kappa})) \mathbf{U}_{2\kappa} = \mathbf{U}_{2\kappa}^{\text{inc}}, \\
 (\mathbf{I} - \mathbf{B}_{3\kappa}(\mathbf{U}_\kappa, \mathbf{U}_{2\kappa}, \mathbf{U}_{3\kappa})) \mathbf{U}_{3\kappa} = \mathbf{C}_{3\kappa}(\mathbf{U}_\kappa, \mathbf{U}_{2\kappa}) + \mathbf{U}_{3\kappa}^{\text{inc}},
 \end{cases} \tag{21}$$

where $\{z_l\}_{l=1}^N$ is a discrete set of nodes such that $-2\pi\delta =: z_1 < z_2 < \dots < z_l < \dots < z_N =: 2\pi\delta$.

$\mathbf{U}_{n\kappa} := \{U_l(n\kappa)\}_{l=1}^N \approx \{U(n\kappa; z_l)\}_{l=1}^N$ denotes the vector of the unknown approximate solution values corresponding to the frequencies $n\kappa$, $n = 1, 2, 3$. The matrices are of the form

$$\mathbf{B}_{n\kappa}(\mathbf{U}_\kappa, \mathbf{U}_{2\kappa}, \mathbf{U}_{3\kappa}) = \{A_m K_{lm}(n\kappa, \mathbf{U}_\kappa, \mathbf{U}_{2\kappa}, \mathbf{U}_{3\kappa})\}_{l,m=1}^N$$

with entries

$$\begin{aligned} K_{lm}(n\kappa, \mathbf{U}_\kappa, \mathbf{U}_{2\kappa}, \mathbf{U}_{3\kappa}) := & -\frac{i(n\kappa)^2}{2\Gamma_{n\kappa}} \exp(i\Gamma_{n\kappa}|z_l - z_m|) \left[1 - \left\{ \varepsilon^{(L)}(z_m) \right. \right. \\ & + \alpha(z_m) \left(|U_m(\kappa)|^2 + |U_m(2\kappa)|^2 + |U_m(3\kappa)|^2 \right. \\ & + \delta_{n1} |U_m(\kappa)| |U_m(3\kappa)| \exp\{i[-3\arg U_m(\kappa) + \arg U_m(3\kappa)]\} \\ & \left. \left. + \delta_{n2} |U_m(\kappa)| |U_m(3\kappa)| \exp\{i[-2\arg U_m(2\kappa) + \arg U_m(\kappa) + \arg U_m(3\kappa)]\} \right) \right\} \Big]. \end{aligned} \quad (22)$$

The numbers A_m are the coefficients determined by the quadrature rule, $\mathbf{I} := \{\delta_{lm}\}_{l,m=1}^N$ is the identity matrix, and δ_{lm} is Kronecker's symbol.

The right-hand side of (21) is defined by

$$\mathbf{U}_{n\kappa}^{\text{inc}} := \{a_{n\kappa}^{\text{inc}} \exp[-i\Gamma_{n\kappa}(z_l - 2\pi\delta)]\}_{l=1}^N,$$

$$\mathbf{C}_\kappa(\mathbf{U}_{2\kappa}, \mathbf{U}_{3\kappa}) := \left\{ \frac{i\kappa^2}{2\Gamma_\kappa} \sum_{m=1}^N A_m \exp(i\Gamma_\kappa|z_l - z_m|) \alpha(z_m) U_m^2(2\kappa) \bar{U}_m(3\kappa) \right\}_{l=1}^N,$$

$$\mathbf{C}_{3\kappa}(\mathbf{U}_\kappa, \mathbf{U}_{2\kappa}) := \left\{ \frac{i(3\kappa)^2}{2\Gamma_{3\kappa}} \sum_{m=1}^N A_m \exp(i\Gamma_{3\kappa}|z_l - z_m|) \alpha(z_m) \left[\frac{1}{3} U_m^3(\kappa) + U_m^2(2\kappa) \bar{U}_m(\kappa) \right] \right\}_{l=1}^N.$$

Given a relative error tolerance $\xi > 0$, the solution of (21) is approximated by means of the following iterative method:

$$\left\{ \begin{aligned} & \left\{ \left[\mathbf{I} - \mathbf{B}_\kappa \left(\mathbf{U}_\kappa^{(s-1)}, \mathbf{U}_{2\kappa}^{(S_2(q))}, \mathbf{U}_{3\kappa}^{(S_3(q))} \right) \right] \mathbf{U}_\kappa^{(s)} \right. \\ & \quad \left. = \mathbf{C}_\kappa \left(\mathbf{U}_{2\kappa}^{(S_2(q))}, \mathbf{U}_{3\kappa}^{(S_3(q))} \right) + \mathbf{U}_\kappa^{\text{inc}} \right\}_{s=1}^{S_1(q): \eta_1(S_1(q)) < \xi} \\ & \left\{ \left[\mathbf{I} - \mathbf{B}_{2\kappa} \left(\mathbf{U}_\kappa^{(S_1(q))}, \mathbf{U}_{2\kappa}^{(s-1)}, \mathbf{U}_{3\kappa}^{(S_3(q))} \right) \right] \mathbf{U}_{2\kappa}^{(s)} = \mathbf{U}_{2\kappa}^{\text{inc}} \right\}_{s=1}^{S_2(q): \eta_2(S_2(q)) < \xi} \\ & \left\{ \left[\mathbf{I} - \mathbf{B}_{3\kappa} \left(\mathbf{U}_\kappa^{(S_1(q))}, \mathbf{U}_{2\kappa}^{(S_2(q))}, \mathbf{U}_{3\kappa}^{(s-1)} \right) \right] \mathbf{U}_{3\kappa}^{(s)} \right. \\ & \quad \left. = \mathbf{C}_{3\kappa} \left(\mathbf{U}_\kappa^{(S_1(q))}, \mathbf{U}_{2\kappa}^{(S_2(q))} \right) + \mathbf{U}_{3\kappa}^{\text{inc}} \right\}_{s=1}^{S_3(q): \eta_3(S_3(q)) < \xi} \end{aligned} \right\}_{q=1}^Q \quad (23)$$

with $\eta_n(s) := \|\mathbf{U}_{n\kappa}^{(s)} - \mathbf{U}_{n\kappa}^{(s-1)}\| / \|\mathbf{U}_{n\kappa}^{(s)}\|$, $n = 1, 2, 3$, where the terminating index $Q \in \mathbb{N}$ is defined by the requirement

$$\max \{\eta_1(Q), \eta_2(Q), \eta_3(Q)\} < \xi.$$

4. Eigen-modes of the linearised problems of scattering and generation of waves on the cubically polarisable layer

The solution of the system of nonlinear equations (19) is approximated by the solution of a linearised system, for given values of the induced dielectric permittivity and of the source functions at the right-hand side of the system. The solution can be found by the help of algorithm (23), where at each step a system of linearised nonlinear complex-valued algebraic equations of the second kind is solved iteratively. The analytic continuation of the linearised nonlinear problems into the region of complex values of the frequency parameter allows us to switch to the analysis of spectral problems. That is, the eigen-frequencies and the corresponding eigen-fields of the homogeneous linear problems with an induced nonlinear permittivity are to be determined. The results of the development of a spectral theory of linear problems for structures with noncompact boundaries can be found in [23], [13], [16], [12], [18], [17].

As mentioned above, the classical formulation of the problem of scattering and generation of waves, described by the *system* of boundary value problems (13), (C1) – (C4), can be reformulated as a *set* of independent spectral problems in the following way:

Find the eigen-frequencies κ_n and the corresponding eigen-functions $E_1(\mathbf{r}, \kappa_n)$ (i.e. $\{\kappa_n \in \Omega_{n\kappa} \subset H_{n\kappa}, E_1(\mathbf{r}, \kappa_n)\}_{n=1}^3$, where $\Omega_{n\kappa}$ are the discrete sets of eigen-frequencies lying on the two-sheeted Riemann surfaces $H_{n\kappa}$, see Fig. 2 and the more detailed explanations below) satisfying the equations

$$\nabla^2 E_1(\mathbf{r}, \kappa_n) + \kappa_n^2 \varepsilon_{n\kappa}(z, \alpha(z), E_1(r, \kappa), E_1(\mathbf{r}, 2\kappa), E_1(\mathbf{r}, 3\kappa)) E_1(\mathbf{r}, \kappa_n) = 0, \quad n = 1, 2, 3, \quad (24)$$

together with the following conditions:

- (CS1) $E_1(\kappa_n; y, z) = U(\kappa_n; z) \exp(i\phi_{n\kappa}y)$, $n = 1, 2, 3$
 (the quasi-homogeneity condition w.r.t. the spatial variable y),
- (CS2) $\phi_{n\kappa} = n\phi_\kappa$, $n = 1, 2, 3$
 (the condition of phase synchronism of waves),
- (CS3) $\mathbf{E}_{\text{tg}}(\kappa_n; y, z)$ and $\mathbf{H}_{\text{tg}}(\kappa_n; y, z)$ (i.e. $E_1(\kappa_n; y, z)$ and $H_2(\kappa_n; y, z)$) are continuous at the boundary layers of the structure with the *induced* permittivity $\varepsilon_{n\kappa}$ for $\kappa := \kappa^{\text{inc}}$, $n = 1, 2, 3$,
- (CS4) $E_1(\kappa_n; y, z) = \begin{cases} a_{\kappa_n} \\ b_{\kappa_n} \end{cases} \exp(i(\phi_{n\kappa}y \pm \Gamma_{\kappa_n}(\kappa_n, \phi_{n\kappa})(z \mp 2\pi\delta)))$, $z \gtrless \pm 2\pi\delta$, $n = 1, 2, 3$
 (the radiation condition w.r.t. the eigen-field).

For real values of the parameters κ_n and $\phi_{n\kappa}$, the condition (CS4) meets the physically reasonable requirement of the absence of radiation fields of waves coming from infinity $z = \pm\infty$:

$$\Im \Gamma_{\kappa_n}(\kappa_n, \phi_{n\kappa}) \geq 0, \quad \Re \Gamma_{\kappa_n}(\kappa_n, \phi_{n\kappa}) \Re \kappa_n \geq 0 \quad \text{for} \quad \Im \phi_{n\kappa} = 0, \quad \Im \kappa_n = 0, \quad n = 1, 2, 3. \quad (25)$$

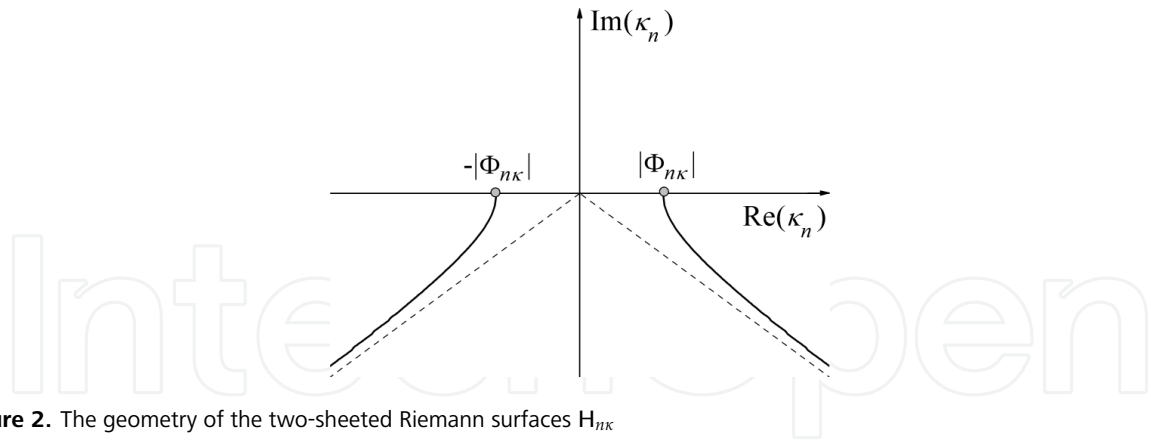


Figure 2. The geometry of the two-sheeted Riemann surfaces $H_{n\kappa}$

The nontrivial solutions (eigen-fields) of problem (24), (CS1) – (CS4) can be represented as

$$E_1(\kappa_n; y, z) = U(\kappa_n; z) \exp(i\phi_{n\kappa}y) = \begin{cases} a_{\kappa_n} \exp(i(\phi_{n\kappa}y + \Gamma_{\kappa_n}(\kappa_n, \phi_{n\kappa})(z - 2\pi\delta))), & z > 2\pi\delta, \\ U(\kappa_n; z) \exp(i\phi_{n\kappa}y), & |z| \leq 2\pi\delta, \\ b_{\kappa_n} \exp(i(\phi_{n\kappa}y - \Gamma_{\kappa_n}(\kappa_n, \phi_{n\kappa})(z + 2\pi\delta))), & z < -2\pi\delta, \end{cases} \quad \kappa_n \in \Omega_{n\kappa} \subset H_{n\kappa}, \quad n = 1, 2, 3, \quad (26)$$

where $\kappa := \kappa^{\text{inc}}$ is a given constant equal to the value of the excitation frequency of the nonlinear structure, $\Gamma_{\kappa_n}(\kappa_n, \phi_{n\kappa}) := (\kappa_n^2 - \phi_{n\kappa}^2)^{1/2}$ are the transverse propagation functions depending on the complex frequency spectral variables κ_n , $\phi_{n\kappa} := n\kappa \sin(\varphi_{n\kappa})$ denote the given real values of the longitudinal propagation constants, $\varepsilon_{n\kappa} = \varepsilon_{n\kappa}(z, \alpha(z), E_1(\mathbf{r}, \kappa), E_1(\mathbf{r}, 2\kappa), E_1(\mathbf{r}, 3\kappa))$ are the induced dielectric permittivities at the frequencies $n\kappa$ corresponding to the parameter $\kappa := \kappa^{\text{inc}}$, $\Omega_{n\kappa}$ are the sets of eigen-frequencies and $H_{n\kappa}$ are two-sheeted Riemann surfaces (cf. Fig. 2), $n = 1, 2, 3$. The range of the spectral parameters $\kappa_n \in \Omega_{n\kappa}$ is completely determined by the boundaries of those regions in which the analytic continuation (consistent with the condition (25)) of the canonical Green's functions

$$G_0(\kappa_n; q, q_0) = \frac{i}{4Y} \exp\{i[\phi_{n\kappa}(y - y_0) + \Gamma_{\kappa_n}(\kappa_n, \phi_{n\kappa})|z - z_0|]\} / \Gamma_{\kappa_n}(\kappa_n, \phi_{n\kappa}), \quad n = 1, 2, 3,$$

into the complex space of the spectral parameters κ_n of the unperturbed problems (24), (CS1) – (CS4) (i.e. for the special case $\varepsilon_{n\kappa} \equiv 1$, $n = 1, 2, 3$) is possible. These complex spaces are two-sheeted Riemann surfaces $H_{n\kappa}$ (see Fig. 2) with real algebraic branch points of second order κ_n^\pm : $\Gamma_{\kappa_n}(\kappa_n^\pm, \phi_{n\kappa}) = 0$ (i.e. $\kappa_n^\pm = \pm|\phi_{n\kappa}|$, $n = 1, 2, 3$) and with cuts starting at these points and extending along the lines

$$(\Re \kappa_n)^2 - (\Im \kappa_n)^2 - \phi_{n\kappa}^2 = 0, \quad \Im \kappa_n \leq 0, \quad n = 1, 2, 3. \quad (27)$$

The first, “physical” sheets (i.e. the pair of values $\{\kappa_n, \Gamma_{\kappa_n}(\kappa_n, \phi_{n\kappa})\}$) on each of the surfaces $H_{n\kappa}$, $n = 1, 2, 3$, are completely determined by the condition (25) and the cuts (27). At the first sheets of $H_{n\kappa}$ the signs of the pairs $\{\kappa_n, \Re \Gamma_{\kappa_n}\}$ and $\{\kappa_n, \Im \Gamma_{\kappa_n}\}$ are distributed as follows: $\Im \Gamma_{\kappa_n} > 0$ for $0 < \arg \kappa_n < \pi$, $\Re \Gamma_{\kappa_n} \geq 0$ for $0 < \arg \kappa_n < \pi/2$ and $\Re \Gamma_{\kappa_n} \leq 0$ for

$\pi/2 \leq \arg \kappa_n < \pi$. For points κ_n with $3\pi/2 \leq \arg \kappa_n \leq 2\pi$, the function values (where $(\Re \kappa_n)^2 - (\Im \kappa_n)^2 - \phi_{n\kappa^2} > 0$) are determined by the condition $\Im \Gamma_{\kappa_n} < 0, \Re \Gamma_{\kappa_n} > 0$, for the remaining points κ_n the function $\Gamma_{\kappa_n}(\kappa_n, \phi_{n\kappa})$ is determined by the condition $\Im \Gamma_{\kappa_n} > 0, \Re \Gamma_{\kappa_n} \leq 0$. In the region $\pi < \arg \kappa_n < 3\pi/2$ the situation is similar to the previous one up to the change of the sign of $\Re \Gamma_{\kappa_n}$. The second, “unphysical” sheets of the surfaces $H_{n\kappa}, n = 1, 2, 3$ are different from the “physical” ones in that, for each κ_n , the signs of both $\Re \Gamma_{\kappa_n}$ and $\Im \Gamma_{\kappa_n}$ are reversed.

The qualitative analysis of the eigen-modes of the linearised problems (24), (CS1) – (CS4) is carried out using the equivalent formulation of spectral problems for the linearised nonlinear integral equations (19). It is based on the analytic continuation of (19) into the space of spectral values $\kappa_n \in \Omega_{n\kappa} \subset H_{n\kappa}, n = 1, 2, 3$.

The spectral problem reduces to finding nontrivial solutions $U(\kappa_n; z)$ of a set of homogeneous (i.e. with vanishing right-hand sides), linear (i.e. linearised equations (19)) integral equations with the induced dielectric permittivity at the frequencies $n\kappa$ of excitation and generation:

$$U(\kappa_n; z) + \frac{i\kappa_n^2}{2\Gamma_{\kappa_n}(\kappa_n, \phi_{n\kappa})} \int_{-2\pi\delta}^{2\pi\delta} \exp(i\Gamma_{\kappa_n}(\kappa_n, \phi_{n\kappa})|z - z_0|) \times [1 - \varepsilon_{n\kappa}(z_0, \alpha(z_0), U(2\kappa; z_0), U(3\kappa; z_0))] U(\kappa_n; z_0) dz_0 = 0; \quad (28)$$

$$|z| \leq 2\pi\delta, \quad \kappa := \kappa^{\text{inc}}, \quad \kappa_n \in \Omega_{n\kappa} \subset H_{n\kappa}, \quad n = 1, 2, 3.$$

The solution of the problem (24), (CS1) – (CS4) can be obtained from the solution of the equivalent problem (28), where – according to (CS3) – in the representation of the eigen-fields (26) the following formulas are used:

$$U(\kappa_n; 2\pi\delta) = a_{\kappa_n}, \quad U(\kappa_n; -2\pi\delta) = b_{\kappa_n}, \quad n = 1, 2, 3. \quad (29)$$

The qualitative analysis of the spectral characteristics allows to develop algorithms for solving the spectral problems (24), (CS1) – (CS4) by reducing them to the equivalent spectral problem of finding nontrivial solutions of the integral equations (28), see [13], [23]. The solvability of (28) follows from an analysis of the basic qualitative characteristics of the spectra. Applying to the integral equations (28) appropriate quadrature formulas, we obtain a set of independent systems of linear algebraic equations of second kind depending nonlinearly on the spectral parameter: $(\mathbf{I} - \mathbf{B}_{n\kappa}(\kappa_n))\mathbf{U}_{\kappa_n} = \mathbf{0}$, where $\kappa_n \in H_{n\kappa}, \kappa := \kappa^{\text{inc}}, n = 1, 2, 3$. Consequently, the spectral problem of finding the eigen-frequencies $\kappa_n \in \Omega_{n\kappa} \subset H_{n\kappa}$ and the corresponding eigen-fields (i.e. the nontrivial solutions of the integral equations (28)) reduces to the following algorithm:

$$\begin{cases} f_{n\kappa}(\kappa_n) := \det(\mathbf{I} - \mathbf{B}_{n\kappa}(\kappa_n)) = 0, \\ (\mathbf{I} - \mathbf{B}_{n\kappa}(\kappa_n))\mathbf{U}_{\kappa_n} = \mathbf{0}, \\ \kappa := \kappa^{\text{inc}}, \quad \kappa_n \in \Omega_{n\kappa} \subset H_{n\kappa}, \quad n = 1, 2, 3. \end{cases} \quad (30)$$

Here we use a similar notation to that in Section 3. κ_n are the desired eigen-frequencies, and $\mathbf{U}_{\kappa_n} = \{U(\kappa_n; z_l)\}_{l=1}^N := \{U_l(\kappa_n)\}_{l=1}^N$ are the vectors of the unknown approximate solution

values corresponding to the frequencies κ_n . The matrices are of the form

$$\mathbf{B}_{n\kappa}(\kappa_n) := \mathbf{B}_{n\kappa}(\kappa_n; \mathbf{U}_\kappa, \mathbf{U}_{2\kappa}, \mathbf{U}_{3\kappa}) = \{A_m K_{lm}(\kappa_n, \mathbf{U}_\kappa, \mathbf{U}_{2\kappa}, \mathbf{U}_{3\kappa})\}_{l,m=1}^N \quad (31)$$

with *given* values of the vectors of the scattered and generated fields $\mathbf{U}_{n\kappa} = \{U(n\kappa; z_l)\}_{l=1}^N := \{U_l(n\kappa)\}_{l=1}^N$, $n = 1, 2, 3$. The numbers A_m are the coefficients determined by the quadrature rule, and the entries $K_{lm}(\kappa_n, \mathbf{U}_\kappa, \mathbf{U}_{2\kappa}, \mathbf{U}_{3\kappa})$ are calculated by means of (22), where the first argument $n\kappa$ is replaced by κ_n . The eigen-frequencies $\kappa_n \in \Omega_{n\kappa} \subset \mathbf{H}_{n\kappa}$, $n = 1, 2, 3$, i.e. the characteristic numbers of the dispersion equations of the problem (30), are obtained by solving the corresponding dispersion equations $f_{n\kappa}(\kappa_n) := \det(\mathbf{I} - \mathbf{B}_{n\kappa}(\kappa_n)) = 0$ by the help of Newton's method or its modifications. The nontrivial solutions \mathbf{U}_{κ_n} of the homogeneous systems of linear algebraic equations (30) corresponding to these characteristic numbers are the eigen-fields (26) of the linearised nonlinear layered structures with an induced dielectric constant. Since the solutions \mathbf{U}_{κ_n} are unique up to multiplication by an arbitrary constant, we require $U(\kappa_n; 2\pi\delta) = a_{\kappa_n} := 1$ (cf. (26)). According to (31), the matrix entries in (30) depend on the dielectric permittivities. The latter are defined by the scattered and generated fields $\mathbf{U}_\kappa, \mathbf{U}_{2\kappa}, \mathbf{U}_{3\kappa}$ of the problem (19) by means of the algorithm (23). This defines the basic design of the implemented numerical algorithm. The investigation of the eigen-modes of the linearised nonlinear structures (30) should always precede the solution of the nonlinear scattering and generation problem in the self-consistent formulation (23). Note that, in the analysis of the linear structures, the problem of excitation (scattering) and the spectral problem can be solved independently.

5. Numerical examples

Consider the excitation of the nonlinear structure by a strong incident field at the basic frequency κ and, in addition, by weak incident quasi-homogeneous electromagnetic fields at the double and triple frequencies $2\kappa, 3\kappa$ (see (12)), i.e.

$$0 < \max\{|a_{2\kappa}^{\text{inc}}|, |a_{3\kappa}^{\text{inc}}|\} \ll |a_{1\kappa}^{\text{inc}}|. \quad (32)$$

The desired solution of the scattering and generation problem (13), (C1) – (C4) (or of the equivalent problems (16) and (19)) are represented as in (15). According to (17) we determine the values of complex amplitudes $\{a_{n\kappa}^{\text{scat}}, b_{n\kappa}^{\text{scat}} : n = 1, 2, 3\}$ in (15) for the scattered and generated fields by means of the formulas (20). The solution of (21) is obtained by means of successive approximations using the self-consistent approach based on the iterative algorithm (23).

In order to describe the scattering and generation properties of the nonlinear structure in the zones of reflection $z > 2\pi\delta$ and transmission $z < -2\pi\delta$, we introduce the following notation:

$$R_{n\kappa} := |a_{n\kappa}^{\text{scat}}|^2 / \sum_{n=1}^3 |a_{n\kappa}^{\text{inc}}|^2 \quad \text{and} \quad T_{n\kappa} := |b_{n\kappa}^{\text{scat}}|^2 / \sum_{n=1}^3 |a_{n\kappa}^{\text{inc}}|^2, \quad n = 1, 2, 3.$$

The quantities $R_{n\kappa}, T_{n\kappa}$ are called *reflection, transmission or generation coefficients* of the waves w.r.t. the total intensity of the incident packet.

We note that, for nonabsorbing media with $\Im[\varepsilon^{(L)}(z)] = 0$, the energy balance equation

$$\sum_{n=1}^3 [R_{n\kappa} + T_{n\kappa}] = 1 \quad (33)$$

is satisfied. This equation generalises the law of conservation of energy which has been treated in [12], [21] for the case of a single incident field and a single equation. If we define by

$$W_{n\kappa} := |a_{n\kappa}^{\text{scat}}|^2 + |b_{n\kappa}^{\text{scat}}|^2 \quad (34)$$

the total energy of the scattered and generated fields at the frequencies $n\kappa$, $n = 1, 2, 3$, then the energy balance equation (33) can be rewritten as

$$\sum_{n=1}^3 W_{n\kappa} = \sum_{n=1}^3 |a_{n\kappa}^{\text{inc}}|^2.$$

In the numerical experiments, the quantities $W_{3\kappa}/W_{\kappa}$ (which characterises the portion of energy generated in the third harmonic in comparison to the energy scattered in the nonlinear layer) and

$$W^{(\text{Error})} := 1 - \sum_{n=1}^3 [R_{n\kappa} + T_{n\kappa}] \quad (35)$$

(which characterises the numerical violation of the energy balance) are of particular interest. We emphasize that in the numerical simulation of scattering and generation processes without any weak fields, i.e. $a_{2\kappa}^{\text{inc}} = a_{3\kappa}^{\text{inc}} = 0$, the residual of the energy balance equation (33) does not exceed the value $|W^{(\text{Error})}| < 10^{-8}$. However, taking into consideration the impact of weak fields in the numerical simulation of the same scattering and generation processes, i.e. $a_{n\kappa}^{\text{inc}} \neq 0$, $n = 2, 3$, the error in the balance equation (33) can reach up to several percent. This indicates that the intensities of the exciting weak fields are sufficiently large such that these fields become also sources for the generation of oscillations. For such situations, the presented mathematical model (13), (C1) – (C4) and (24), (CS1) – (CS4) should take into account the complex Fourier amplitudes of the oscillations at the frequencies $n\kappa$ for numbers $n > 3$. Furthermore we observe, on the one hand, situations in which the influence of a weak field $a_{2\kappa}^{\text{inc}} \neq 0$ on the scattering and generation process of oscillations leads to small errors in the energy balance equation (33) not exceeding 2% (that is $|W^{(\text{Error})}| < 0.02$), and, on the other hand, situations in which the error can reach 10% (that is $|W^{(\text{Error})}| < 0.1$). The scattering, generating, energetic, and dielectric properties of the nonlinear layer are illustrated by surfaces in dependence on the parameters of the particular problem. The bottom chart depicts the surface of the value of the residual $W^{(\text{Error})}$ of the energy balance equation (see (35)) and its projection onto the top horizontal plane of the figure. In particular, by the help of these graphs it is easy to localise that region of parameters of the problem, where the error of the energy balance does not exceed a given value, that is $|W^{(\text{Error})}| < \text{const}$.

The spectral characteristics of the linearised nonlinear problems (24), (CS1) – (CS4) with the induced dielectric permittivity (11) at the frequencies $n\kappa$, $n = 1, 2, 3$, of excitation and

generation were calculated by means of the algorithm (30). In the graphical illustration of the eigen-fields U_{κ_n} in the representation (26) we have set $a_{\kappa_n} := 1$ for $\kappa_n \in \Omega_{n\kappa} \subset H_{n\kappa}$, $n = 1, 2, 3$. Finally we mention that the later-used classification of scattered, generated or eigen-fields of the dielectric layer by the $H_{m,l,p}$ -type is identical to that given in [12], [13], [23]. In the case of E-polarisation, see (3), $H_{m,l,p}$ (or $TE_{m,l,p}$) denotes the type of polarisation of the wave field under investigation. The subscripts indicate the number of local maxima of $|E_1|$ (or $|U|$, as $|E_1| = |U|$, see (15), (26)) along the coordinate axes x , y and z (see Fig. 1). Since the considered waves are homogeneous along the x -axis and quasi-homogeneous along the y -axis, we study actually fields of the type $H_{0,0,p}$ (or $TE_{0,0,p}$), where the subscript p is equal to the number of local maxima of the function $|U|$ of the argument $z \in [-2\pi\delta, 2\pi\delta]$.

In what follows we present and discuss results of the numerical analysis of scattering and generation properties as well as the eigen-modes of the dielectric layer with a positive value of the cubic susceptibility of the medium. In more detail, we consider a single-layered structure with a dielectric permittivity $\varepsilon_{n\kappa}(z, \alpha(z), U(\kappa; z), U(2\kappa; z), U(3\kappa; z)) = \varepsilon^{(L)}(z) + \varepsilon_{n\kappa}^{(NL)}$, $n = 1, 2, 3$, where $\varepsilon^{(L)}(z) := 16$ and $\alpha(z) := 0.01$ for $z \in [-2\pi\delta, 2\pi\delta]$, $\varepsilon_{n\kappa}^{(NL)}$ is given by (11), $\delta := 0.5$, $\kappa^{\text{inc}} := \kappa := 0.375$, and $\varphi_\kappa \in [0^\circ, 90^\circ]$. The Figs. 3 – Fig. 13 illustrate the following cases of the incident fields:

- $a_{2\kappa}^{\text{inc}} = \frac{1}{3}a_\kappa^{\text{inc}}, a_{3\kappa}^{\text{inc}} = 0 \quad \dots$ graphs labeled by "1/3",
- $a_{2\kappa}^{\text{inc}} = \frac{2}{3}a_\kappa^{\text{inc}}, a_{3\kappa}^{\text{inc}} = 0 \quad \dots$ graphs labeled by "2/3",
- $a_{2\kappa}^{\text{inc}} = a_{3\kappa}^{\text{inc}} = 0 \quad \dots$ graphs labeled by "0".

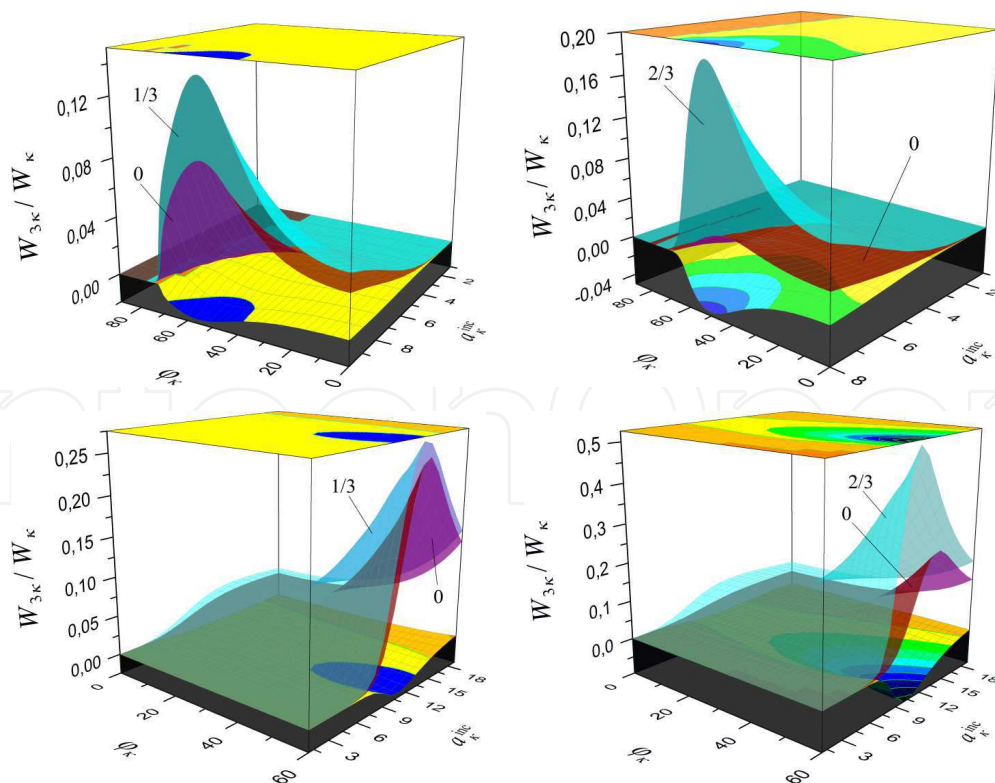


Figure 3. The portion of energy generated in the third harmonic: $a_{2\kappa}^{\text{inc}} = \frac{1}{3}a_\kappa^{\text{inc}}$ (left), $a_{2\kappa}^{\text{inc}} = \frac{2}{3}a_\kappa^{\text{inc}}$ (right)

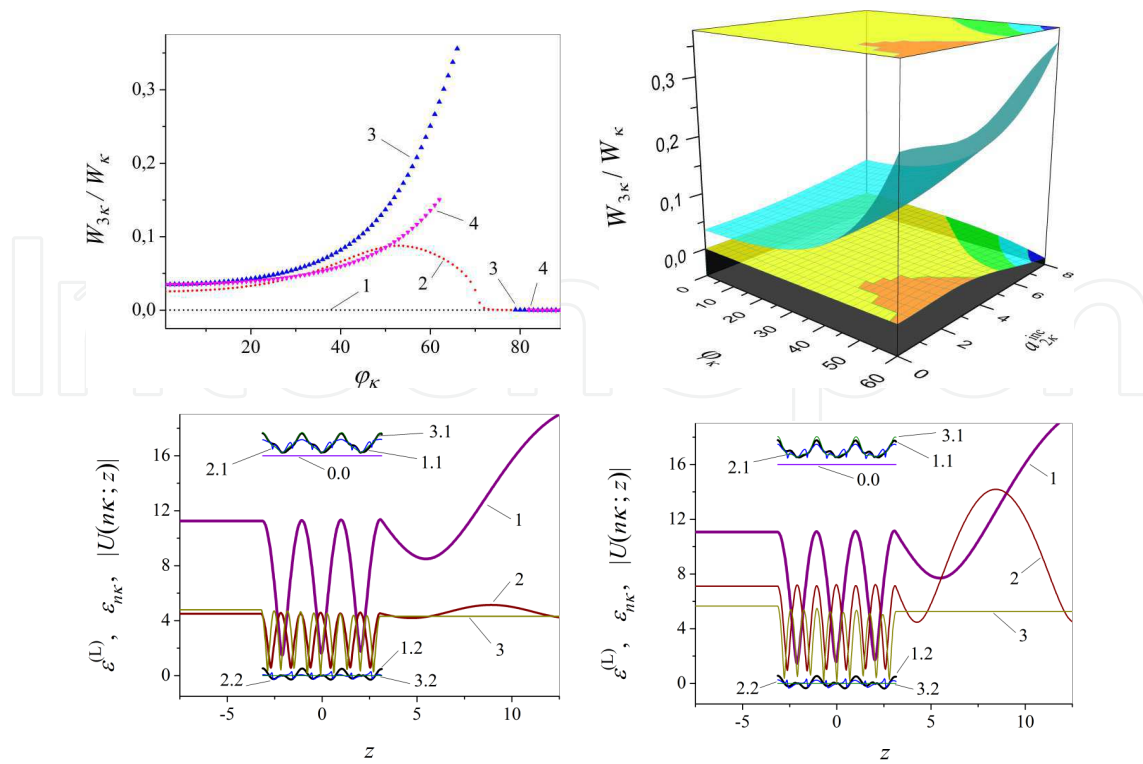


Figure 4. The portion of energy generated in the third harmonic: #1 ... $a_{\kappa}^{inc} = 1$, #2 ... $a_{\kappa}^{inc} = 9.93$, #3 ... $a_{\kappa}^{inc} = 14$, #4 ... $a_{\kappa}^{inc} = 19$ for $a_{2\kappa}^{inc} = 0$ (top left), the dependence of $W_{3\kappa}/W_{\kappa}$ on φ_{κ} , $a_{2\kappa}^{inc}$ for $a_{\kappa}^{inc} = 14$ (top right), some graphs describing the properties of the non-linear layer for $\varphi_{\kappa} = 60^\circ$, $a_{\kappa}^{inc} = 14$ and $a_{2\kappa}^{inc} = \frac{1}{3}a_{\kappa}^{inc}$ (bottom left), $a_{2\kappa}^{inc} = \frac{2}{3}a_{\kappa}^{inc}$ (bottom right): #0.0 ... $\varepsilon^{(L)}$, #1 ... $|U(\kappa; z)|$, #2 ... $|U(2\kappa; z)|$, #3 ... $|U(3\kappa; z)|$, #n.1 ... $\Re \varepsilon(\varepsilon_{n\kappa})$, #n.2 ... $\Im \varepsilon(\varepsilon_{n\kappa})$

The results shown in Fig. 3 allow us to track the dynamic behaviour of the quantity $W_{3\kappa}/W_{\kappa}$ characterising the ratio of the generated and scattered energies. Fig. 3 shows the dependence of $W_{3\kappa}/W_{\kappa}$ on the angle of incidence φ_{κ} and on the amplitude a_{κ}^{inc} of the incident field for different relations between $a_{2\kappa}^{inc}$ and a_{κ}^{inc} . It describes the portion of energy generated in the third harmonic by the nonlinear layer when a plane wave at the excitation frequency κ and with the amplitude a_{κ}^{inc} is passing the layer under the angle of incidence φ_{κ} . It can be seen that the weaker incident field at the frequency 2κ leads to an increase of $W_{3\kappa}/W_{\kappa}$ in comparison with the situation where the structure is excited only by a single field at the basic frequency κ . For example, in Fig. 3 the maximum value of $W_{3\kappa}/W_{\kappa}$ and the value $W^{(Error)}$ are reached at the following parameters $[a_{\kappa}^{inc}, a_{2\kappa}^{inc}, \varphi_{\kappa}]$: $W_{3\kappa}/W_{\kappa} = 0.08753$, $W^{(Error)} = -1.98292 \cdot 10^{-9}$, $[a_{\kappa}^{inc} = 9.93, a_{2\kappa}^{inc} = 0, \varphi_{\kappa} = 53^\circ]$... graph #0 and, taking into consideration the weak field at the double frequency, $W_{3\kappa}/W_{\kappa} = 0.13903$, $W^{(Error)} = -0.01692$, $[a_{\kappa}^{inc} = 9.93, a_{2\kappa}^{inc} = \frac{1}{3}a_{\kappa}^{inc}, \varphi_{\kappa} = 53^\circ]$... graph #1/3 (top left); $W_{3\kappa}/W_{\kappa} = 0.03265$, $W^{(Error)} = -8.53239 \cdot 10^{-9}$, $[a_{\kappa}^{inc} = 8, a_{2\kappa}^{inc} = 0, \varphi_{\kappa} = 42^\circ]$... graph #0 and, taking into consideration the weak field at the double frequency, $W_{3\kappa}/W_{\kappa} = 0.1864$, $W^{(Error)} = -0.04625$, $[a_{\kappa}^{inc} = 8, a_{2\kappa}^{inc} = \frac{2}{3}a_{\kappa}^{inc}, \varphi_{\kappa} = 50^\circ]$... graph #2/3 (top right); $W_{3\kappa}/W_{\kappa} = 0.25054$, $W^{(Error)} = -9.29243 \cdot 10^{-10}$, $[a_{\kappa}^{inc} = 14, a_{2\kappa}^{inc} = 0, \varphi_{\kappa} = 60^\circ]$... graph #0 (bottom left and right) and, taking into consideration the weak field at the double frequency, $W_{3\kappa}/W_{\kappa} = 0.26589$, $W^{(Error)} = -0.00578$, $[a_{\kappa}^{inc} = 14, a_{2\kappa}^{inc} = \frac{1}{3}a_{\kappa}^{inc}, \varphi_{\kappa} = 60^\circ]$... graph #1/3 (bottom left); $W_{3\kappa}/W_{\kappa} = 0.42662$, $W^{(Error)} = -0.06037$ $[a_{\kappa}^{inc} = 13, a_{2\kappa}^{inc} = \frac{2}{3}a_{\kappa}^{inc}, \varphi_{\kappa} = 60^\circ]$... graph #2/3 (bottom right).

The numerical analysis of the processes displayed in Fig. 4 (top left) by the curves #3 in the range of angles $\varphi_\kappa \in (66^\circ, 79^\circ)$ and #4 in the range of angles $\varphi_\kappa \in (62^\circ, 82^\circ)$ did not lead to the convergence of the computational algorithm. The value $W_{3\kappa}/W_\kappa = 0.3558$ for $a_\kappa^{\text{inc}} = 14$, $a_{2\kappa}^{\text{inc}} = 0$ and $\varphi_\kappa = 66^\circ$ (see the graph #3 in Fig. 4 (top left)) indicates that $W_{3\kappa}$ is 35.58% of W_κ . This is the maximal value of $W_{3\kappa}/W_\kappa$ that has been achieved in the case of a single incident field at the basic frequency κ . Fig. 4 (top right) illustrates the portion of energy generated in the third harmonic in dependence on the angle of incidence φ_κ and on the amplitude $a_{2\kappa}^{\text{inc}}$ of the incident field at the double frequency. Here the maximum value of $W_{3\kappa}/W_\kappa$ is reached at $[a_\kappa^{\text{inc}} = 14, a_{2\kappa}^{\text{inc}} = 8, \varphi_\kappa = 60^\circ]$. If the structure is excited by a single field at the basic frequency κ only, then the portion of energy generated in the third harmonic is $\approx 25.05\%$, i.e. for $[a_\kappa^{\text{inc}} = 14, a_{2\kappa}^{\text{inc}} = 0, \varphi_\kappa = 60^\circ]$ we have $W_{3\kappa}/W_\kappa = 0.25054$ and $W^{(\text{Error})} = -9.29243 \cdot 10^{-10}$. If we take into consideration the weak exciting field at the double frequency, then we get for $[a_\kappa^{\text{inc}} = 14, a_{2\kappa}^{\text{inc}} = 8, \varphi_\kappa = 60^\circ]$ the following results: $W_{3\kappa}/W_\kappa = 0.35084$ and $W^{(\text{Error})} = -0.0377$ (which corresponds to a relative error of 3.78% in the energy balance).

The bottom diagrams in Fig. 4 display some graphs characterising the scattering and generation properties of the nonlinear structure. Graph #0.0 illustrates the value of the linear part $\varepsilon^{(L)} = 16$ of the permittivity of the nonlinear layered structure. Graphs #n.1 and #n.2 show the real and imaginary parts of the permittivities at the frequencies $n\kappa$, $n = 1, 2, 3$. The figure also shows the absolute values $|U(\kappa; z)|$, $|U(2\kappa; z)|$ of the amplitudes of the full scattered fields at the frequencies of excitation κ , 2κ (graphs #1, #2) and $|U(3\kappa; z)|$ of the generated field at the frequency 3κ (graph #3). The values $|U(n\kappa; z)|$ are given in the nonlinear layered structure ($|z| \leq 2\pi\delta$) and outside it (i.e. in the zones of reflection $z > 2\pi\delta$ and transmission $z < -2\pi\delta$). Here $W^{(\text{Error})} = -5.782328 \cdot 10^{-3}$, i.e. the error in the energy balance is less than 0.58% (bottom left) and $W^{(\text{Error})} = -4.567534 \cdot 10^{-2}$, i.e. the error in the energy balance is less than 4.57% (bottom right).

Figs. 5 and 6 show the numerical results obtained for the scattered and the generated fields in the nonlinear structure and for the residual $W^{(\text{Error})}$ of the energy balance equation (33) for an incident angle $\varphi_\kappa = 60^\circ$ in dependence on the amplitudes a_κ^{inc} and $a_{2\kappa}^{\text{inc}}$ of the plane incident waves at the basic frequency κ and at the double frequency 2κ , resp. The figures show the graphs of $|U_{n\kappa}[a_\kappa^{\text{inc}}, a_{2\kappa}^{\text{inc}}, z]|$, $n = 1, 2, 3$, demonstrating the dynamic behaviour of the scattered and the generated fields $|U(n\kappa; z)|$ in the nonlinear layered structure in dependence on increasing amplitudes a_κ^{inc} and $a_{2\kappa}^{\text{inc}}$ for an incident angle $\varphi_\kappa = 60^\circ$ of the plane waves. We mention that, in the range $a_\kappa^{\text{inc}} \in (0, 22]$ and $a_{2\kappa}^{\text{inc}} = \frac{1}{3}a_\kappa^{\text{inc}}$ (see Fig. 5) or $a_{2\kappa}^{\text{inc}} = \frac{2}{3}a_\kappa^{\text{inc}}$ (see Fig. 6) of the amplitudes of the incident fields and for an incident angle $\varphi_\kappa = 60^\circ$ of the plane waves, the scattered field has the type $H_{0,0,4}$ at the frequency κ and $H_{0,0,7}$ at the frequency 2κ . The generated field, observed in the range $a_\kappa^{\text{inc}} \in [5, 22]$, is of the type $H_{0,0,10}$ at the frequency 3κ , see Figs. 5, 6 (bottom left).

The nonlinear parts $\varepsilon_{n\kappa}^{(NL)}$ of the dielectric permittivity at each frequency $n\kappa$ depend on the values $U_{n\kappa} := U(n\kappa; z)$, $n = 1, 2, 3$, of the fields. The variation of the nonlinear parts $\varepsilon_{n\kappa}^{(NL)}$ of the dielectric permittivity for increasing amplitudes a_κ^{inc} and $a_{2\kappa}^{\text{inc}}$ of the incident fields are illustrated by the behaviour of $\Re(\varepsilon_{n\kappa}[a_\kappa^{\text{inc}}, a_{2\kappa}^{\text{inc}}, z])$ and $\Im(\varepsilon_{n\kappa}[a_\kappa^{\text{inc}}, a_{2\kappa}^{\text{inc}}, z])$ at the frequencies $n\kappa$ in Fig. 7 (case $a_{2\kappa}^{\text{inc}} = \frac{1}{3}a_\kappa^{\text{inc}}$) and Fig. 8 (case $a_{2\kappa}^{\text{inc}} = \frac{2}{3}a_\kappa^{\text{inc}}$). The quantities $\Im(\varepsilon_{n\kappa})$ take both positive and negative values along the height of the nonlinear layer (i.e.

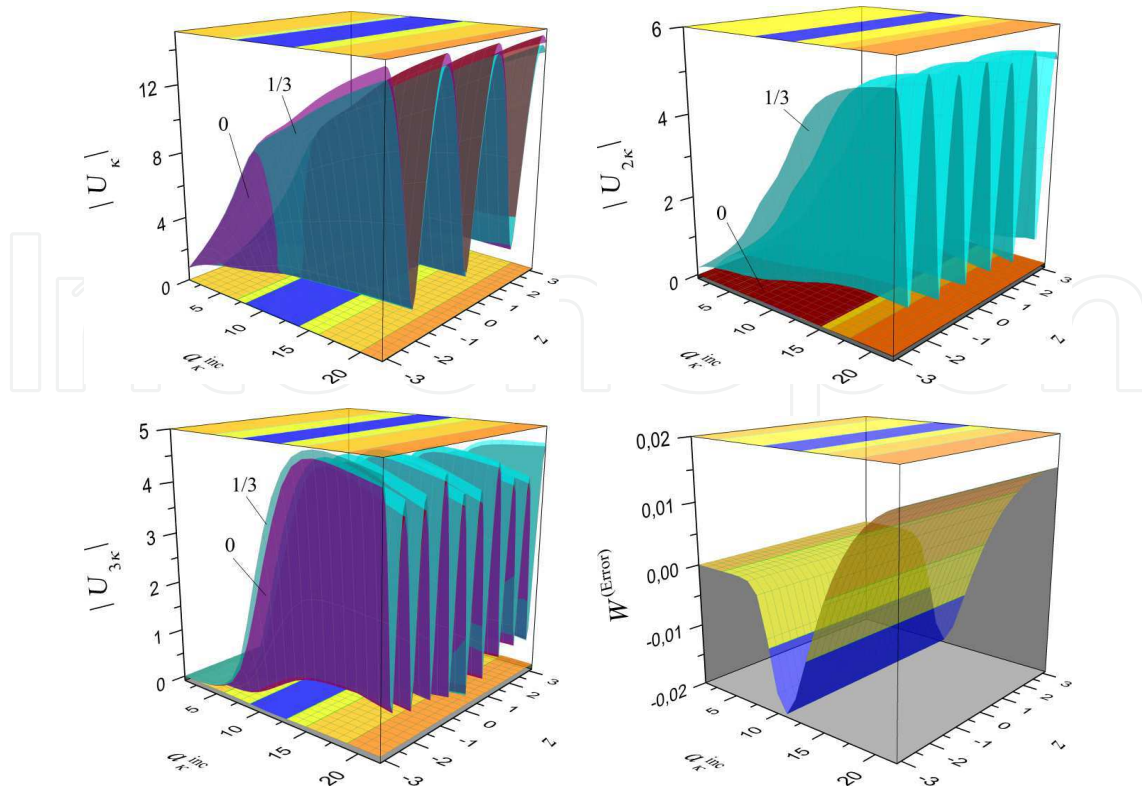


Figure 5. Graphs of the scattered and generated fields in the nonlinear layered structure in dependence on $[a_{\kappa}^{\text{inc}}, a_{2\kappa}^{\text{inc}}, z]$ for $\varphi_{\kappa} = 60^{\circ}$ and $a_{2\kappa}^{\text{inc}} = \frac{1}{3}a_{\kappa}^{\text{inc}}$: $|U_{\kappa}|$ (top left), $|U_{2\kappa}|$ (top right) $|U_{3\kappa}|$ (bottom left), and the residual $W^{(\text{Error})}$ of the energy balance equation (bottom right)

in the interval $z \in [-2\pi\delta, 2\pi\delta]$, see Figs. 7, 8 (right). For given amplitudes a_{κ}^{inc} and $a_{2\kappa}^{\text{inc}}$, the graph of $\Im(\varepsilon_{n\kappa}[a_{\kappa}^{\text{inc}}, a_{2\kappa}^{\text{inc}}, z])$ characterises the *loss of energy* in the nonlinear layer at the excitation frequencies $n\kappa$, $n = 1, 2$, caused by the *generation* of the electromagnetic field of the third harmonic. Such a situation arises because of the right-hand side of (13) at the triple frequency and the generation which is evoked by the right-hand side of (13) at the basic frequency. In our case $\Im[\varepsilon^{(L)}(z)] = 0$ and $\Im[\alpha(z)] = 0$, therefore, according to (11),

$$\begin{aligned} & \Im(\varepsilon_{n\kappa}(z, \alpha(z), U(\kappa; z), U(2\kappa; z), U(3\kappa; z))) \\ &= \alpha(z) [\delta_{n1}|U(\kappa; z)||U(3\kappa; z)|\Im(\exp\{i[-3\arg(U(\kappa; z)) + \arg(U(3\kappa; z))]\}) \\ & \quad + \delta_{n2}|U(\kappa; z)||U(3\kappa; z)|\Im(\exp\{i[-2\arg(U(2\kappa; z)) + \arg(U(\kappa; z)) + \arg(U(3\kappa; z))]\})], \\ & \qquad \qquad \qquad n = 1, 2, 3. \end{aligned} \tag{36}$$

From Figs. 7, 8 (right) we see that small values of a_{κ}^{inc} and $a_{2\kappa}^{\text{inc}}$ induce a small amplitude of the function $\Im(\varepsilon_{n\kappa})$, i.e. $|\Im(\varepsilon_{n\kappa})| \approx 0$. The increase of a_{κ}^{inc} corresponds to a strong incident field and leads to the generation of a third harmonic field $U(3\kappa; z)$, and the increase of $a_{2\kappa}^{\text{inc}}$ changes the behaviour of $\varepsilon_{n\kappa}$ (compare the surface #0 with the surfaces #1/3 and #2/3 in Figs. 7, 8). Figs. 7, 8 (right) show the dynamic behaviour of $\Im(\varepsilon_{n\kappa})$. It can be seen that $\Im(\varepsilon_{3\kappa}) = 0$, whereas at the same time the values of $\Im(\varepsilon_{n\kappa})$, $n = 1, 2$, may be *positive or negative* along the height of the nonlinear layer, i.e. in the interval $z \in [-2\pi\delta, 2\pi\delta]$, see (36).

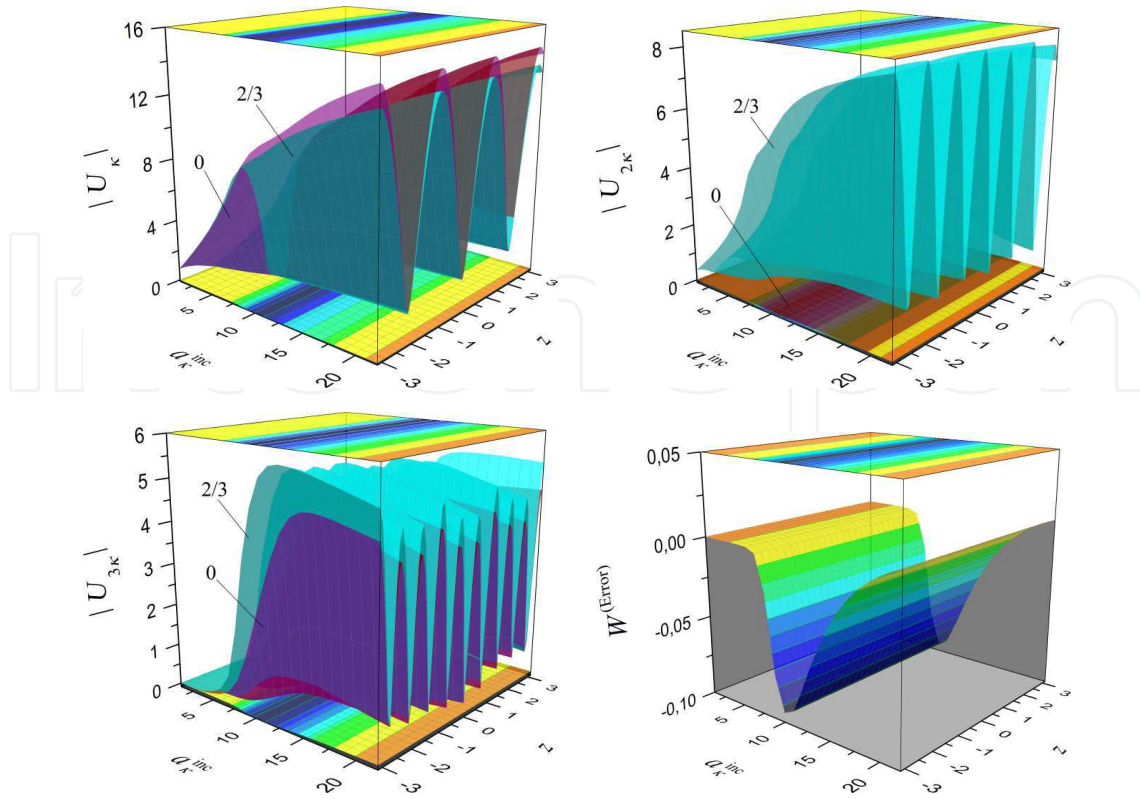


Figure 6. Graphs of the scattered and generated fields in the nonlinear layered structure in dependence on $[a_\kappa^{\text{inc}}, a_{2\kappa}^{\text{inc}}, z]$ for $\varphi_\kappa = 60^\circ$ and $a_{2\kappa}^{\text{inc}} = \frac{2}{3}a_\kappa^{\text{inc}}$: $|U_\kappa|$ (top left), $|U_{2\kappa}|$ (top right), $|U_{3\kappa}|$ (bottom left), and the residual $W^{(\text{Error})}$ (bottom right)

The zero values of $\Im(\varepsilon_{n\kappa})$, $n = 1, 2$, are determined by the phase relations between the scattered and the generated fields in the nonlinear layer, namely at the basic frequency κ by the phase relation between $U(\kappa; z)$, $U(3\kappa; z)$, and at the double frequency 2κ by the phases of $\{U(n\kappa; z)\}_{n=1,2,3}$, see (36):

$$\delta_{n1} [-3\arg(U(\kappa; z)) + \arg(U(3\kappa; z))] + \delta_{n2} [-2\arg(U(2\kappa; z)) + \arg(U(\kappa; z)) + \arg(U(3\kappa; z))] = p\pi, \quad p = 0, \pm 1, \dots, n = 1, 2.$$

We mention that the behaviour of both the quantities $\Im(\varepsilon_{n\kappa})$ and

$$\begin{aligned} & \Re(\varepsilon_{n\kappa}(z, \alpha(z), U(\kappa; z), U(2\kappa; z), U(3\kappa; z)) - \varepsilon_{3\kappa}(z, \alpha(z), U(\kappa; z), U(2\kappa; z), U(3\kappa; z))) \\ &= \alpha(z) [\delta_{n1} |U(\kappa; z)| |U(3\kappa; z)| \Re(\exp\{i[-3\arg(U(\kappa; z)) + \arg(U(3\kappa; z))]\}) \\ & \quad + \delta_{n2} |U(\kappa; z)| |U(3\kappa; z)| \Re(\exp\{i[-2\arg(U(2\kappa; z)) + \arg(U(\kappa; z)) + \arg(U(3\kappa; z))]\})], \\ & \qquad \qquad \qquad n = 1, 2, \end{aligned} \quad (37)$$

plays an essential role in the process of third harmonic generation. Figs. 7, 8 (bottom) show the graphs describing the behaviour of $\Re(\varepsilon_\kappa[a_\kappa^{\text{inc}}, a_{2\kappa}^{\text{inc}}, z] - \varepsilon_{3\kappa}[a_\kappa^{\text{inc}}, a_{2\kappa}^{\text{inc}}, z])$ and $\Re(\varepsilon_{2\kappa}[a_\kappa^{\text{inc}}, a_{2\kappa}^{\text{inc}}, z] - \varepsilon_{3\kappa}[a_\kappa^{\text{inc}}, a_{2\kappa}^{\text{inc}}, z])$.

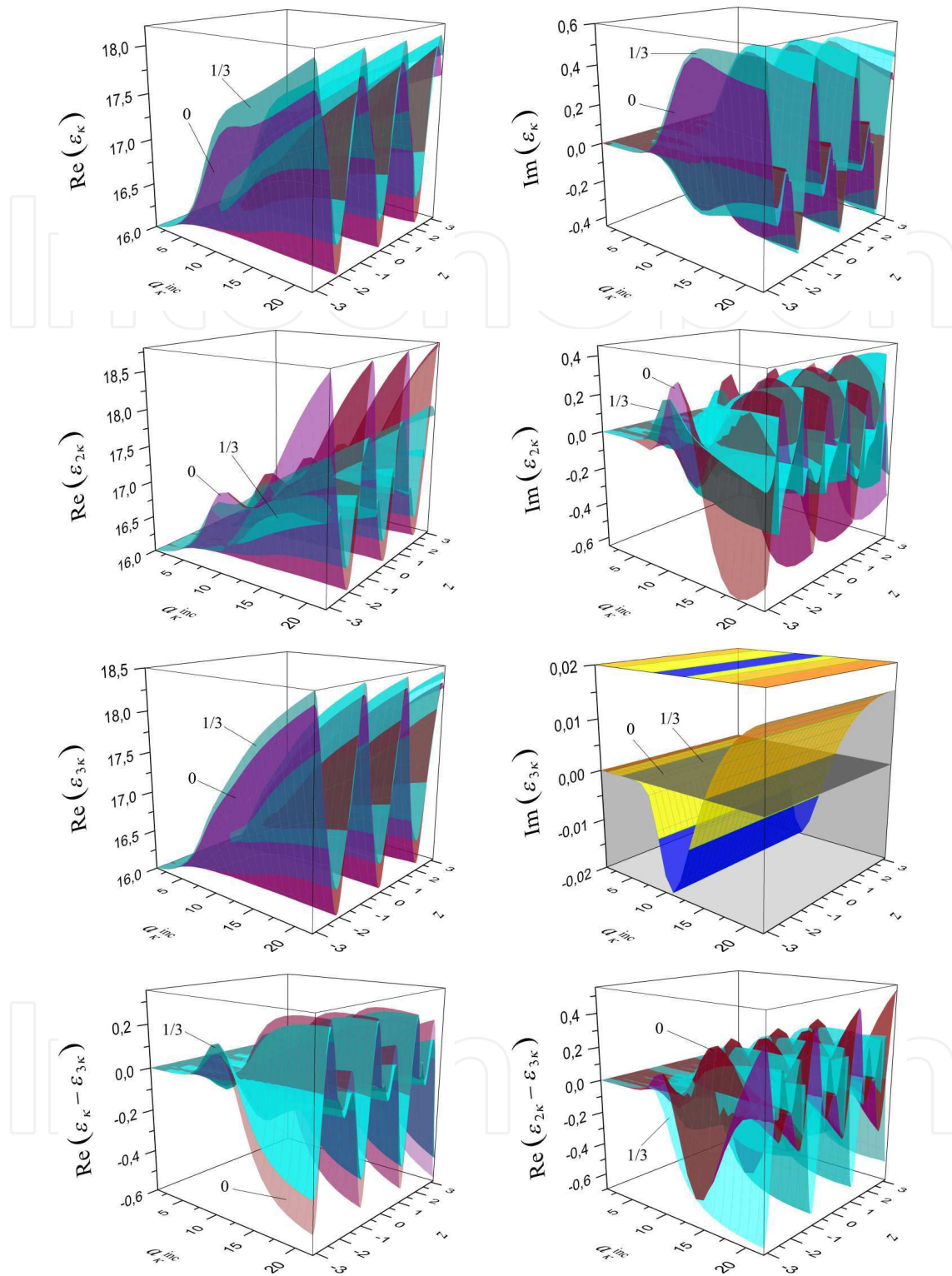


Figure 7. Graphs characterising the nonlinear dielectric permittivity in dependence on $[a_{\kappa}^{\text{inc}}, a_{2\kappa}^{\text{inc}}, z]$ for $\varphi_{\kappa} = 60^{\circ}$ and $a_{2\kappa}^{\text{inc}} = \frac{1}{3}a_{\kappa}^{\text{inc}}$: $\Re \epsilon(\epsilon_{\kappa})$ (top left), $\Im \epsilon(\epsilon_{\kappa})$ (top right), $\Re \epsilon(\epsilon_{2\kappa})$ (second from top left), $\Im \epsilon(\epsilon_{2\kappa})$ (second from top right), $\Re \epsilon(\epsilon_{3\kappa})$ (second to the last left), $\Im \epsilon(\epsilon_{3\kappa})$ (second to the last right), $\Re \epsilon(\epsilon_{\kappa} - \epsilon_{3\kappa})$ (bottom left), $\Re \epsilon(\epsilon_{2\kappa} - \epsilon_{3\kappa})$ (bottom right)

We mention that the impact of a strong electromagnetic field with an amplitude a_{κ}^{inc} even in the absence of a weak field $a_{2\kappa}^{\text{inc}} = 0$ (where $U(2\kappa; z) = 0$, see (11) and the surface #0 in Fig. 5

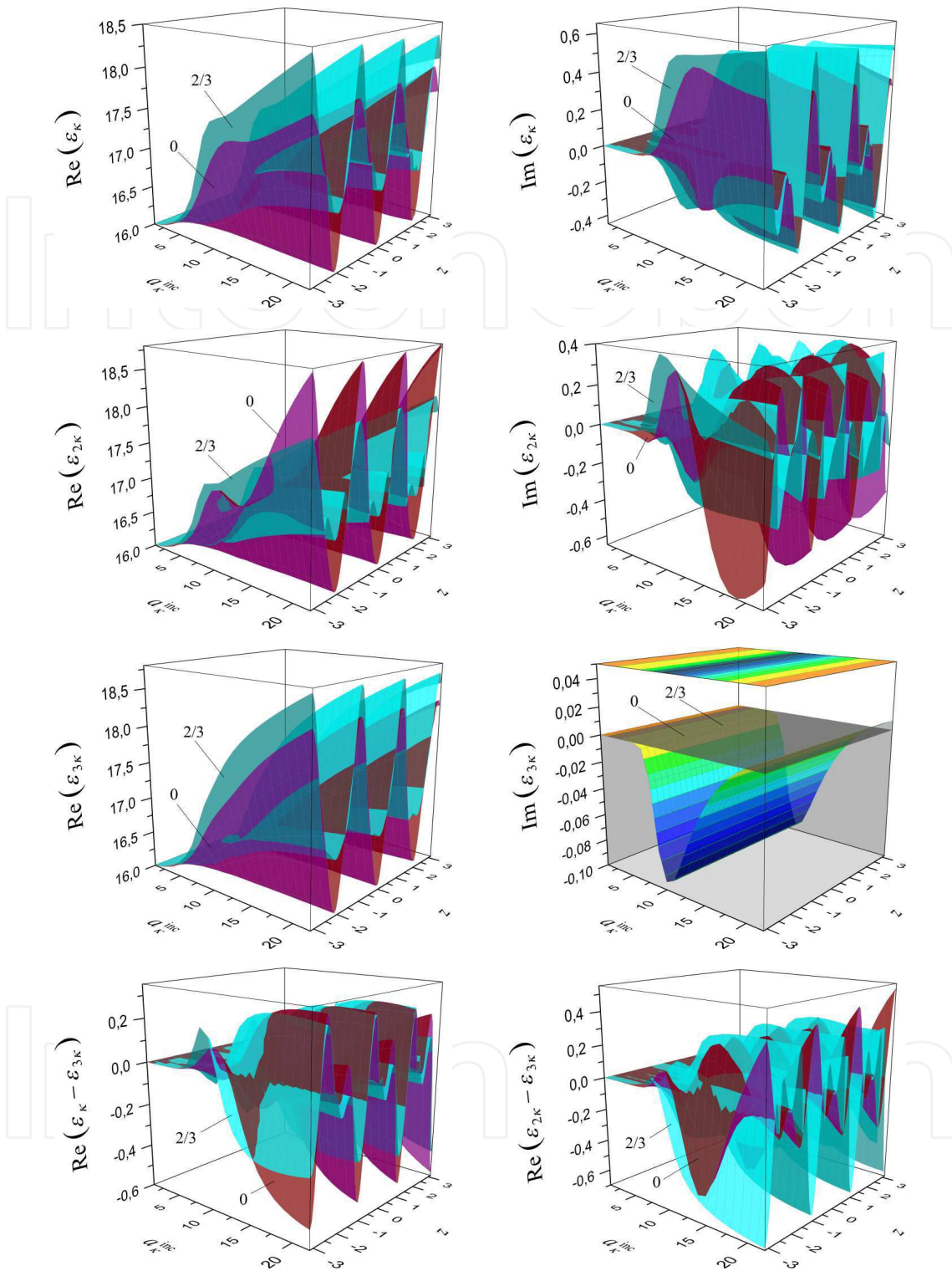


Figure 8. Graphs characterising the nonlinear dielectric permittivity in dependence on $[a_k^{inc}, a_{2k}^{inc}, z]$ for $\varphi_k = 60^\circ$ and $a_{2k}^{inc} = \frac{2}{3}a_k^{inc}$: $\Re \epsilon(\epsilon_\kappa)$ (top left), $\Im \epsilon(\epsilon_\kappa)$ (top right), $\Re \epsilon(\epsilon_{2\kappa})$ (second from top left), $\Im \epsilon(\epsilon_{2\kappa})$ (second from top right), $\Re \epsilon(\epsilon_{3\kappa})$ (second to the last left), $\Im \epsilon(\epsilon_{3\kappa})$ (second to the last right), $\Re(\epsilon_\kappa - \epsilon_{3\kappa})$ (bottom left), $\Re(\epsilon_{2\kappa} - \epsilon_{3\kappa})$ (bottom right)

and Fig. 6 (top right)) induces a nontrivial component of the nonlinear dielectric permittivity at the frequency 2κ . Figs. 7, 8 (second from top) show that the existence of nontrivial values

$\Re(\varepsilon_{2\kappa}) \neq \Re(\varepsilon^{(L)})$ and $\Im(\varepsilon_{2\kappa}) \neq 0$ is caused by the amplitude and phase characteristics of the fields $U(\kappa; z)$ and $U(3\kappa; z)$, see (11) taking into account $U(2\kappa; z) = 0$. Moreover, the nonlinear component of the dielectric permittivity, which is responsible for the variation of $\Re(\varepsilon_{n\kappa} - \varepsilon_{3\kappa})$ and $\Im(\varepsilon_{n\kappa})$, does not depend on the absolute value of the amplitude of the field at the double frequency $|U(2\kappa; z)|$, see (37) and (36). Thus, even a weak field (see (11), #1/3 in Fig. 5 and #2/3 in Fig. 6 (top right)) includes a mechanism for the redistribution of the energy of the incident wave packet which is consumed for the scattering process and the generation of waves, cf. the dynamics of the surfaces #0 with #1/3 and #2/3 in Figs. 5 – 8.

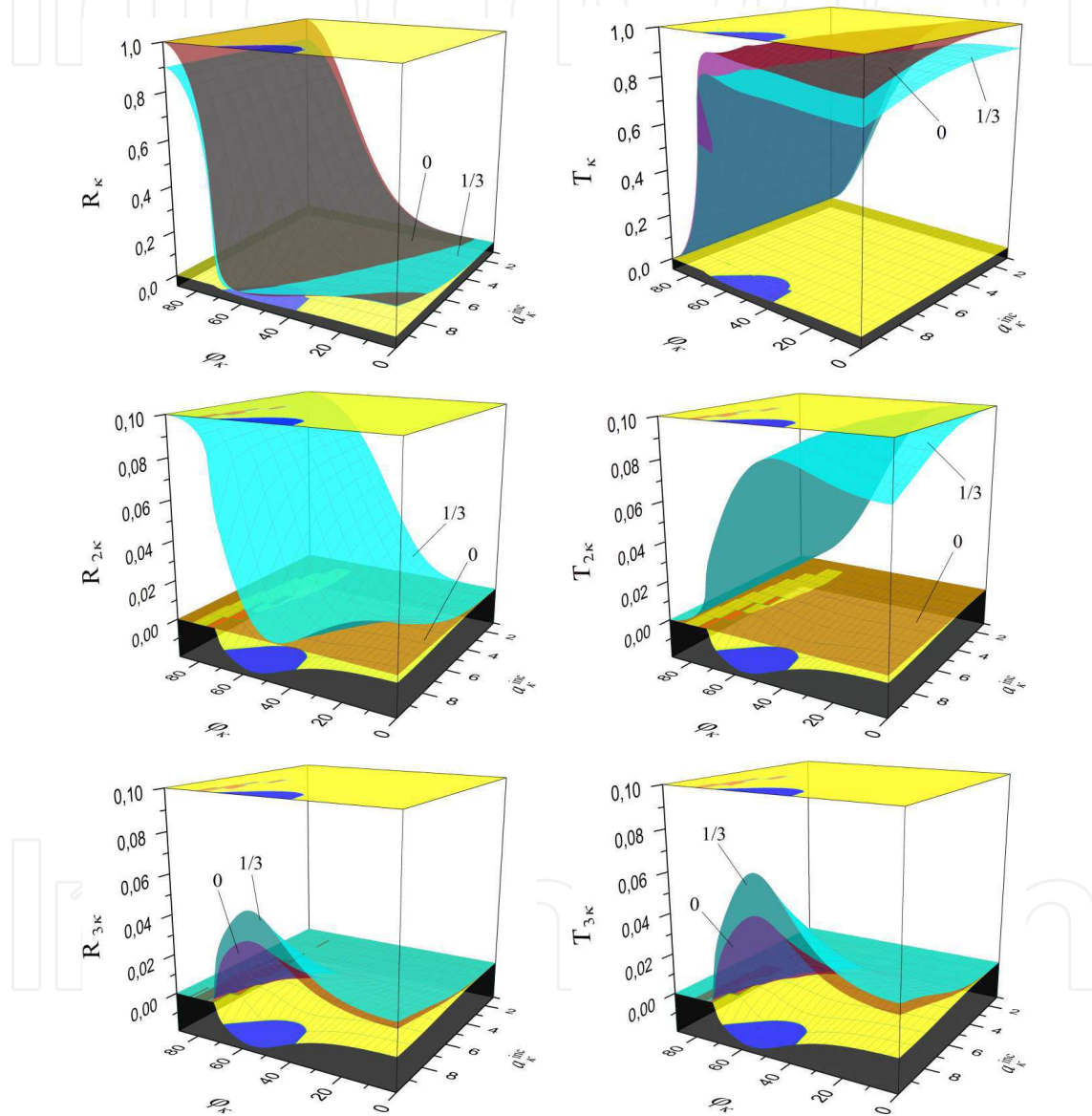


Figure 9. The scattering and generation properties of the nonlinear structure in dependence on $[\varphi_\kappa, a_\kappa^{\text{inc}}, a_{2\kappa}^{\text{inc}}]$ for $a_{2\kappa}^{\text{inc}} = \frac{1}{3}a_\kappa^{\text{inc}}$. R_κ, T_κ (top), $R_{2\kappa}, T_{2\kappa}$ (second from top), $R_{3\kappa}, T_{3\kappa}$ (bottom)

The scattering and generation properties of the nonlinear structure in the ranges $\varphi_\kappa \in [0^\circ, 90^\circ)$, $a_\kappa^{\text{inc}} \in [1, 9.93]$, $a_{2\kappa}^{\text{inc}} = \frac{1}{3}a_\kappa^{\text{inc}}$ and $\varphi_\kappa \in [0^\circ, 90^\circ)$, $a_\kappa^{\text{inc}} \in [1, 8]$ of the parameters of the incident field are presented in Figs. 9 – 11. The graphs show the dynamics of the scattering $(R_\kappa[\varphi_\kappa, a_\kappa^{\text{inc}}, a_{2\kappa}^{\text{inc}}], T_\kappa[\varphi_\kappa, a_\kappa^{\text{inc}}, a_{2\kappa}^{\text{inc}}], R_{2\kappa}[\varphi_\kappa, a_\kappa^{\text{inc}}, a_{2\kappa}^{\text{inc}}], T_{2\kappa}[\varphi_\kappa, a_\kappa^{\text{inc}}, a_{2\kappa}^{\text{inc}}])$, see Figs.

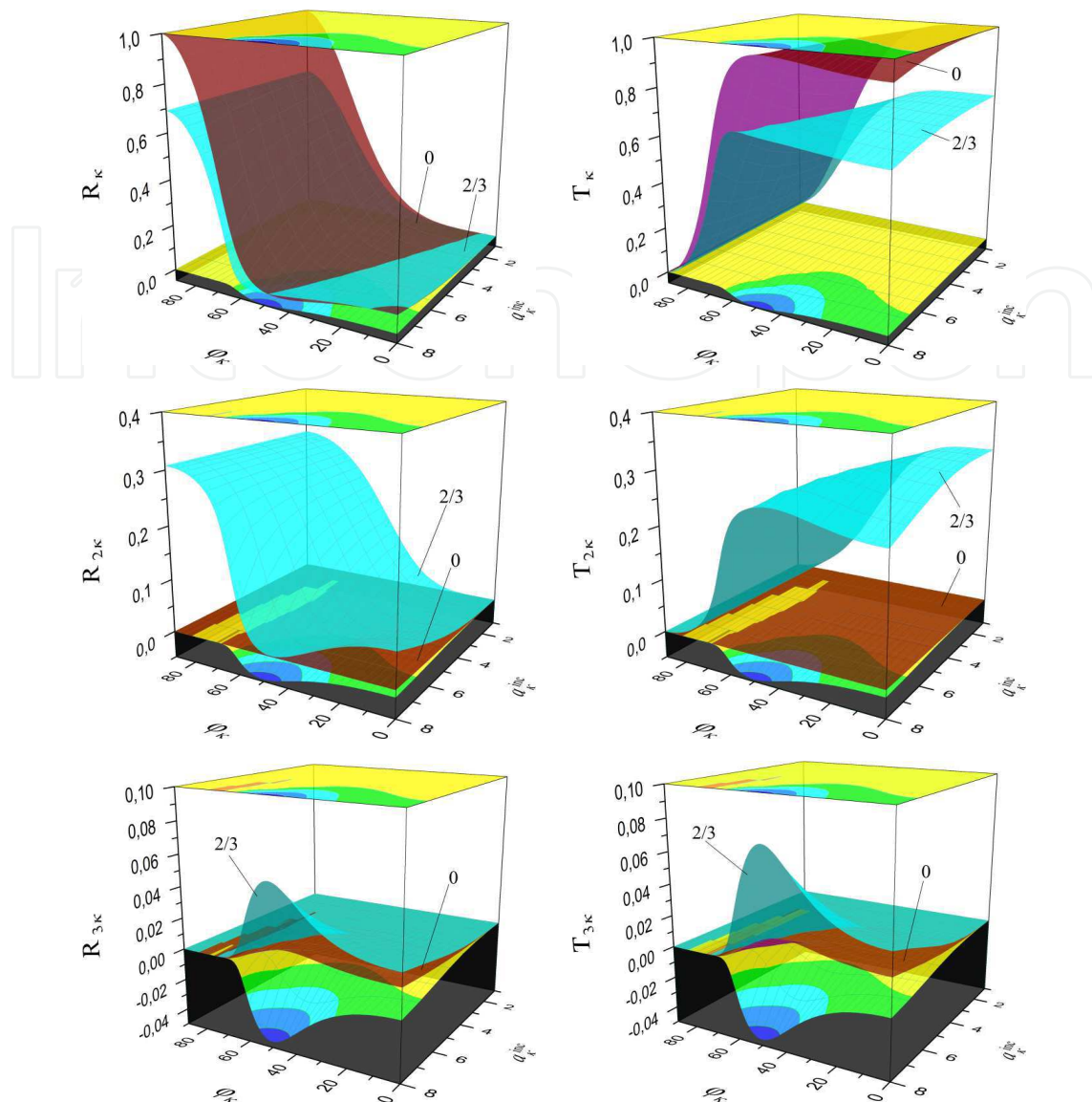


Figure 10. The scattering and generation properties of the nonlinear structure in dependence on $[\varphi_\kappa, a_\kappa^{\text{inc}}, a_{2\kappa}^{\text{inc}}]$ for $a_{2\kappa}^{\text{inc}} = \frac{2}{3} a_\kappa^{\text{inc}}$. R_κ, T_κ (top), $R_{2\kappa}, T_{2\kappa}$ (second from top), $R_{3\kappa}, T_{3\kappa}$ (bottom)

9, 10 (top 2)) and generation ($R_{3\kappa}[\varphi_\kappa, a_\kappa^{\text{inc}}, a_{2\kappa}^{\text{inc}}], T_{3\kappa}[\varphi_\kappa, a_\kappa^{\text{inc}}, a_{2\kappa}^{\text{inc}}]$, see Figs. 9, 10 (bottom)) properties of the structure. Fig. 11 (top) shows cross sections of the surfaces depicted in Fig. 9 and of the graph of $W_{3\kappa}[\varphi_\kappa, a_\kappa^{\text{inc}}, a_{2\kappa}^{\text{inc}}] / W_\kappa[\varphi_\kappa, a_\kappa^{\text{inc}}, a_{2\kappa}^{\text{inc}}]$ (see Fig. 3 (left)) by the planes $\varphi_\kappa = 60^\circ$ and $a_\kappa^{\text{inc}} = 9.93$.

In Figs. 11 – 13, a slightly more detailed illustration for the situation of a single incident field (i.e. $a_{2\kappa}^{\text{inc}} = 0$) is given, cf. also the graphs labeled by “0” in Fig. 9. In the resonant range of wave scattering and generation frequencies, i.e. $\kappa^{\text{scat}} := \kappa^{\text{inc}} = \kappa$ and $\kappa^{\text{gen}} = 3\kappa$, resp., the dynamic behaviour of the characteristic quantities depicted in Figs. 11 – 13 has the following causes. The scattering and generation frequencies are close to the corresponding eigen-frequencies of the linear ($\alpha = 0$) and linearised nonlinear ($\alpha \neq 0$) spectral problems (24), (CS1) – (CS4). Furthermore, the distance between the corresponding eigen-frequencies of the spectral problems with $\alpha = 0$ and $\alpha \neq 0$ is small. Thus, the graphs in Fig. 11 (top)

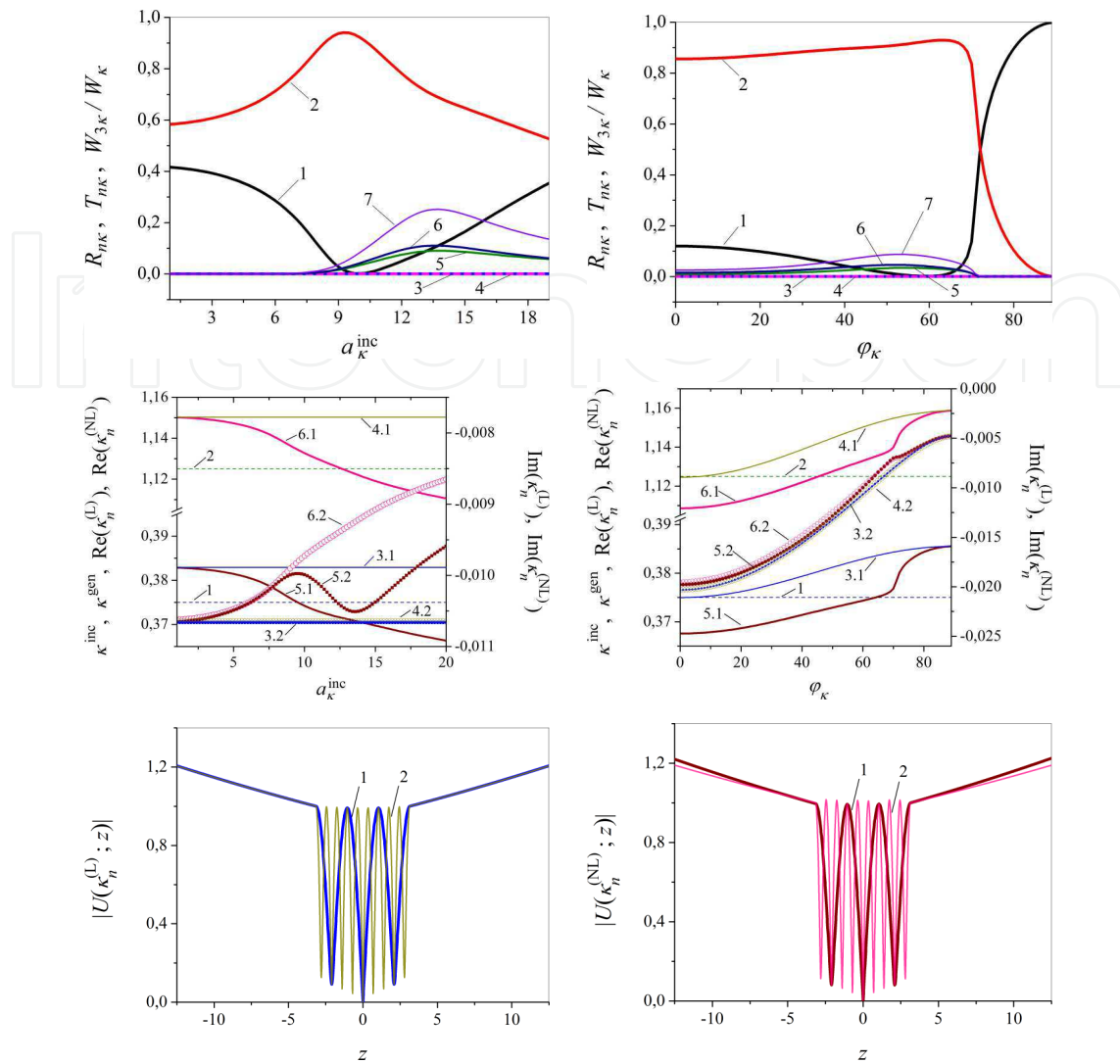


Figure 11. The curves R_κ (#1), T_κ (#2), $R_{2\kappa}$ (#3), $T_{2\kappa}$ (#4), $R_{3\kappa}$ (#5), $T_{3\kappa}$ (#6), $W_{3\kappa}/W_\kappa$ (#7) for $\varphi_\kappa = 60^\circ$ (top left) and $a_\kappa^{\text{inc}} = 9.93$ (top right), the curves $\kappa := \kappa^{\text{inc}} := 0.375$ (#1), $3\kappa = \kappa^{\text{gen}} = 3\kappa^{\text{inc}} = 1.125$ (#2), the complex eigen-frequencies $\Re\epsilon(\kappa_1^{(L)})$ (#3.1), $\Im\epsilon(\kappa_1^{(L)})$ (#3.2), $\Re\epsilon(\kappa_3^{(L)})$ (#4.1), $\Im\epsilon(\kappa_3^{(L)})$ (#4.2) of the linear problem ($\alpha = 0$) and $\Re\epsilon(\kappa_1^{(NL)})$ (#5.1), $\Im\epsilon(\kappa_1^{(NL)})$ (#5.2), $\Re\epsilon(\kappa_3^{(NL)})$ (#6.1), $\Im\epsilon(\kappa_3^{(NL)})$ (#6.2) of the linearised nonlinear problem ($\alpha = +0.01$) for $\varphi_\kappa = 60^\circ$ (second from top left) and $a_\kappa^{\text{inc}} = 9.93$ (second from top right), and the graphs of the eigen-fields of the layer for $\varphi_\kappa = 60^\circ$, $a_\kappa^{\text{inc}} = 14$. The linear problem ($\alpha = 0$, bottom left): $|U(\kappa_1^{(L)}; z)|$ with $\kappa_1^{(L)} = 0.3829155 - i0.01066148$ (#1), $|U(\kappa_3^{(L)}; z)|$ with $\kappa_3^{(L)} = 1.150293 - i0.01062912$ (#2), the linearised nonlinear problem ($\alpha = +0.01$, bottom right): $|U(\kappa_1^{(NL)}; z)|$ with $\kappa_1^{(NL)} = 0.3705110 - i0.01049613$ (#1), $|U(\kappa_3^{(NL)}; z)|$ with $\kappa_3^{(NL)} = 1.121473 - i0.009194824$ (#2)

can be compared with the dynamic behaviour of the branches of the eigen-frequencies of the spectral problems presented in Fig. 11 (second from top). The graphs of the eigen-fields corresponding to the branches of the considered eigen-frequencies are shown in Fig. 11 (bottom).

Fig. 11 (second from top) illustrates the dispersion characteristics of the linear ($\alpha = 0$) and the linearised nonlinear ($\alpha = +0.01$) layer $\epsilon_{n\kappa} = \epsilon^{(L)} + \epsilon_{n\kappa}^{(NL)}$, $n = 1, 2, 3$. The nonlinear components of the permittivity at the scattering (excitation) frequencies $\kappa^{\text{scat}} := \kappa^{\text{inc}} = \kappa$ and the generation frequencies $\kappa^{\text{gen}} := 3\kappa$ depend on the amplitude a_κ^{inc} and the angle of

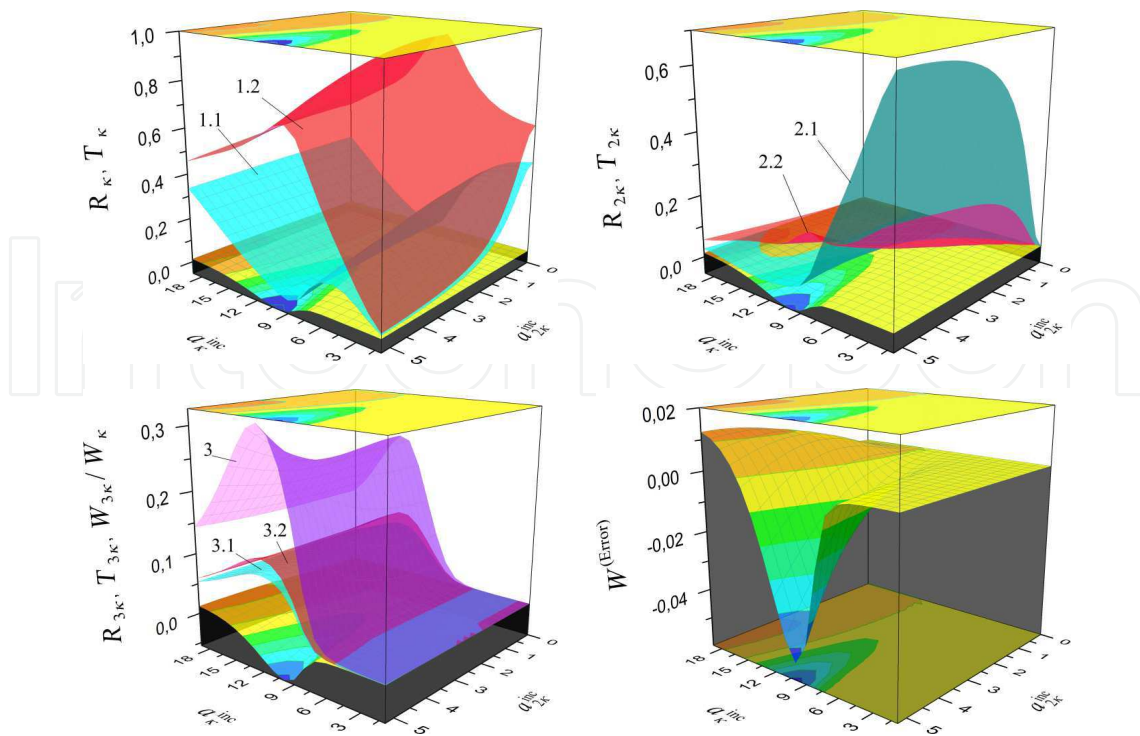


Figure 12. The scattering and generation properties of the nonlinear structure in dependence on $[\varphi_\kappa, a_\kappa^{\text{inc}}, a_{2\kappa}^{\text{inc}}]$ for $\varphi_\kappa = 60^\circ$: R_κ, T_κ (#1.1, #1.2 top left), $R_{2\kappa}, T_{2\kappa}$ (#2.1, #2.2 top right), $W_{3\kappa}/W_\kappa, R_{3\kappa}, T_{3\kappa}$ (#3, #3.1, #3.2 bottom left), $W^{(\text{Error})}$ (bottom right)

incidence φ_κ of the incident field. This is reflected in the dynamics of the behaviour of the complex-valued eigen-frequencies of the linear and the linearised nonlinear layer.

We start the analysis of the results of our calculations with the comparison of the dispersion relations given by the branches of the eigen-frequencies (curves #3.1, #3.2 and #5.1, #5.2) near the scattering frequency (curve #1, corresponding to the excitation frequency) and (curves #4.1, #4.2, #6.1, #6.2) near the oscillation frequency (line #2) in the situations presented in Fig. 11 (second from top). The graph #5.1 lies below the graph #3.1 and the graph #6.1 below the graph #4.1. That is, canalising properties (properties of transparency) of the nonlinear layer occur if $\alpha > 0$. This case is characterised by the increase of the angle of transparency of the nonlinear structure at the excitation frequency with an increasing amplitude of the incident field (see Fig. 9 (top left), there where the reflection coefficient is close to zero). The analysis of the eigen-modes of Fig. 11 (second from top) allows us to explain the mechanisms of the canalisation phenomena (transparency) (see Fig. 9 (top left), Fig. 11 (top, graph #1)) and wave generation (see Fig. 9 (bottom), Fig. 11 (top, graphs #5, #6)).

Comparing the results shown in Fig. 11 (top) and Fig. 11 (second from top) we note the following. The intersection of the curves #1 and #5.1 in Fig. 11 (second from top) defines certain parameters, in the neighborhood of which the canalisation effect (transparency) of the nonlinear structure can be observed in Fig. 11 (top). For example, in Fig. 11 (second from top left) the curves #1 and #5.1 intersect at $a_\kappa^{\text{inc}} = 9.5$, also here the curve #5.2 achieves a local maximum. Near this value, we see the phenomenon of canalisation (transparency) of the layer in Fig. 11 (top left). If we compare the Figs. 11 (top right) and 11 (second from top right), we detect a similar situation. The intersection of the curves #1 and #5.1 defines the parameter

$\varphi_\kappa = 64^\circ$, near which we observe the canalisation effect in Fig. 11 (second from top right). The same is true – to some extent – for the description of the wave generation processes. For example, for similar values of the imaginary parts of the branches of the eigen-frequencies #5.2 and #6.2 in Fig. 11 (second from top right), the intersection of the curves #2 and #6.1 defines the parameter $\varphi_\kappa = 45^\circ$. Near this value, stronger generation properties of the layer can be observed, see Fig. 11 (top) and Fig. 9 (bottom), at $\varphi_\kappa = 45^\circ$. Let us also consider the situation in Fig. 11 (second from top left). Here, at the point of intersection of the curves #2 and #6.1, the graph #5.2 starts to decrease monotonically in some interval. The intersection of the curves #2 and #6.1 defines the parameter $a_\kappa^{\text{inc}} = 12.6$, which falls into the range $[9.5, 13.6]$ of values of the amplitudes at which the curve #5.2 is monotonically decreasing. This leads to a shift in the imaginary part of the eigen-frequency of the scattering structure (graph #5.2) with respect to the eigen-frequency of the generating structure (graph #6.2). The magnitude of the shift depends on the distance between the curves of #6.2 and #5.2 at the given value a_κ^{inc} . The maximal distance between the graphs #6.2 and #5.2 is achieved at the local minimum of the graph #5.2 at $a_\kappa^{\text{inc}} = 13.6$. Right from this point, i.e. with an increasing amplitude a_κ^{inc} , the distance between the graphs #6.2 and #5.2 shows no significant change. The maximum value of the generation is achieved at an amplitude close to the intersection of curves #2 and #6.1, but shifted to the point of the local minimum of the curve #5.2, see $R_{3\kappa}$, $T_{3\kappa}$, $W_{3\kappa}/W_\kappa$ in Fig. 11 (top left), Fig. 9 (bottom) and Fig. 3 (top right).

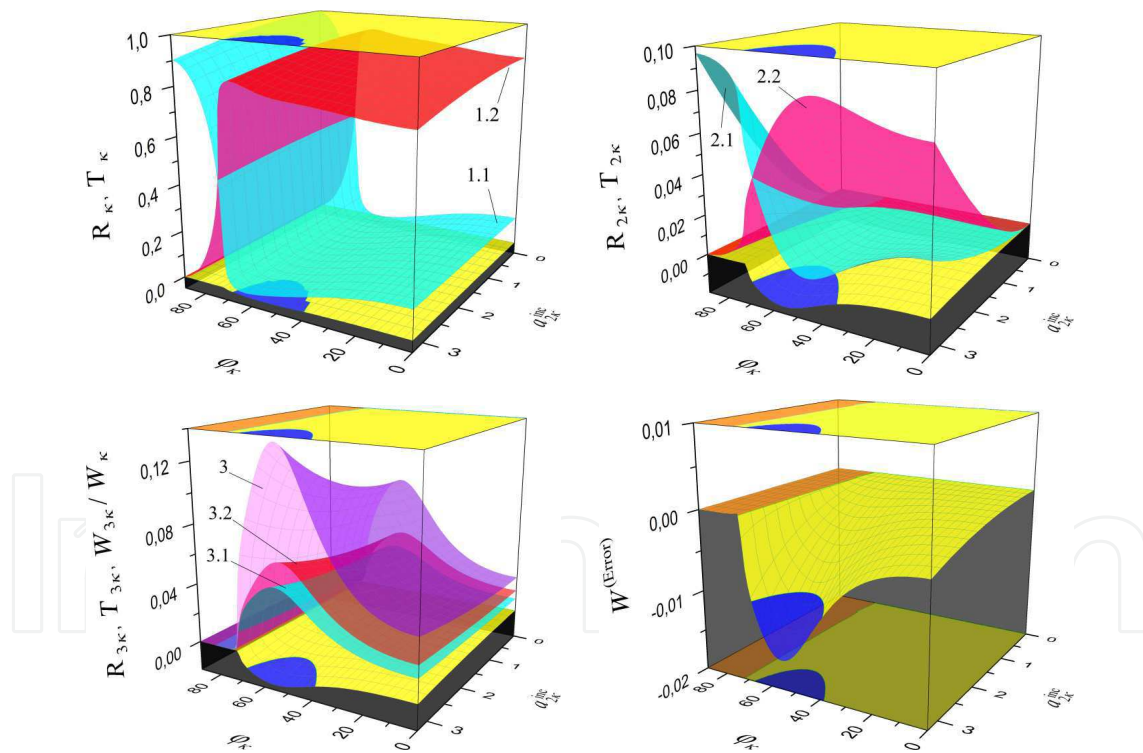


Figure 13. The scattering and generation properties of the nonlinear structure in dependence on $[\varphi_\kappa, a_\kappa^{\text{inc}}, a_{2\kappa}^{\text{inc}}]$ for $a_\kappa^{\text{inc}} = 9.93$: R_κ, T_κ (#1.1, #1.2 top left), $R_{2\kappa}, T_{2\kappa}$ (#2.1, #2.2 top right), $W_{3\kappa}/W_\kappa, R_{3\kappa}, T_{3\kappa}$ (#3, #3.1, #3.2 bottom left), $W^{(\text{Error})}$ (bottom right)

Fig. 11 (bottom) presents the characteristic distribution of the eigen-fields corresponding to the branches of the eigen-frequencies under consideration. The graphs of the eigen-fields of type $H_{0,0,A}$ are labeled by #1, the graphs of the eigen-fields of type $H_{0,0,10}$ by #2.

Figs. 12, 13 show the same dependencies as in Fig. 11 (top) but with the additional parameter $a_{2\kappa}^{\text{inc}}$. Here we can track the dynamics of the scattering, generation and energy characteristics of the nonlinear layer under the influence of the wave package. The incident package consists of a strong and a weak magnetic field with amplitudes a_{κ}^{inc} and $a_{2\kappa}^{\text{inc}}$, resp.

The numerical results presented in this chapter were obtained using an approach based on the description of the wave scattering and generation processes in a nonlinear, cubically polarisable layer by a system of nonlinear integral equations (19), and of the corresponding spectral problems by the nontrivial solutions of the integral equations (28). We have considered an excitation of the nonlinear layer defined by the condition (32). For this case we passed from (19) to (21) and from (28) to (30) by the help of Simpson's quadrature rule. The numerical solution of (21) was obtained using the self-consistent iterative algorithm (23). The problem (30) was solved by means of Newton's method. In the investigated range of parameters, the dimension of the resulting systems of algebraic equations was $N = 301$, and the relative error of calculations did not exceed $\xi = 10^{-7}$.

6. Conclusion

We presented a mathematical model of resonance scattering and generation of waves on an isotropic nonmagnetic nonlinear layered dielectric structure excited by a packet of plane waves in a self-consistent formulation, where the analysis is performed in the domain of resonance frequencies [3, 4, 15]. Here, both the radio [6] and optical [9] frequency ranges are of interest. The wave packets consist of both strong electromagnetic fields at the excitation frequency of the non-linear structure (leading to the generation of waves) and of weak fields at the multiple frequencies (which do not lead to the generation of harmonics but influence on the process of scattering and generation of waves by the non-linear structure). The model reduces to a system of nonlinear boundary-value problems of Sturm-Liouville type or, equivalently, to a system of nonlinear Fredholm integral equations. The solution of these nonlinear problems was obtained rigorously in a self-consistent formulation and without using approximations of the given field, slowly varying amplitudes etc.

The approximate solution of the nonlinear problems was obtained by means of solutions of linear problems with an induced nonlinear dielectric permeability. The analytical continuation of these linear problems into the region of complex values of the frequency parameter allowed us to switch to the analysis of spectral problems. In the frequency domain, the resonant scattering and generation properties of nonlinear structures are determined by the proximity of the excitation frequencies of the nonlinear structures to the complex eigen-frequencies of the corresponding homogeneous linear spectral problems with the induced nonlinear dielectric permeability of the medium.

We presented a collection of numerical results that describe interesting properties of the nonlinear permittivities of the layers as well as their scattering and generation characteristics. The results demonstrate the possibility to control the scattering and generating properties of a nonlinear structure via the intensities of its excitation fields. They also indicate a possibility of designing a frequency multiplier and other electrodynamic devices containing nonlinear dielectrics with controllable permittivity.

Author details

Lutz Angermann¹ and Vasyl V. Yatsyk²

1 Institut für Mathematik, Technische Universität Clausthal, Clausthal-Zellerfeld, Germany

2 Usikov Institute of Radiophysics and Electronics, National Academy of Sciences of Ukraine, Kharkov, Ukraine

References

- [1] Angermann, L. & Yatsyk, V. [2008]. Numerical simulation of the diffraction of weak electromagnetic waves by a Kerr-type nonlinear dielectric layer, *Int. J. Electromagnetic Waves and Electronic Systems* 13(12): 15–30.
- [2] Angermann, L. & Yatsyk, V. [2010]. Mathematical models of the analysis of processes of resonance scattering and generation of the third harmonic by the diffraction of a plane wave through a layered, cubically polarisable structure, *Int. J. Electromagnetic Waves and Electronic Systems* 15(1): 36–49. In Russian.
- [3] Angermann, L. & Yatsyk, V. [2011a]. Generation and resonance scattering of waves on cubically polarisable layered structures, in L. Angermann (ed.), *Numerical Simulations – Applications, Examples and Theory*, InTech, Rijeka/Vienna, Croatia/Austria, pp. 175–212.
- [4] Angermann, L. & Yatsyk, V. [2011b]. Resonance properties of scattering and generation of waves on cubically polarisable dielectric layers, in V. Zhurbenko (ed.), *Electromagnetic Waves*, InTech, Rijeka/Vienna, Croatia/Austria, pp. 299–340.
- [5] Butcher, P. [1965]. Nonlinear optical phenomena, *Bulletin 200*, Ohio State University, Columbus.
- [6] Chernogor, L. [2004]. *Nonlinear Radiophysics*, V.N. Karazin Kharkov National University, Kharkov.
- [7] Kleinman, D. [1962]. Nonlinear dielectric polarization in optical media, *Phys. Rev.* 126(6): 1977–1979.
- [8] Kravchenko, V. & Yatsyk, V. [2007]. Effects of resonant scattering of waves by layered dielectric structure with Kerr-type nonlinearity, *Int. J. Electromagnetic Waves and Electronic Systems* 12(12): 17–40.
- [9] Miloslavsky, V. [2008]. *Nonlinear Optics*, V.N. Karazin Kharkov National University, Kharkov.
- [10] Schürmann, H. W., Serov, V. & Shestopalov, Y. [2001]. Reflection and transmission of a TE-plane wave at a lossless nonlinear dielectric film, *Physica D* 158: 197–215.
- [11] Serov, V., Schürmann, H. & Svetogorova, E. [2004]. Integral equation approach to reflection and transmission of a plane te-wave at a (linear/nonlinear) dielectric film with spatially varying permittivities, *J. Phys. A: Math. Gen.* 37: 3489–3500.

- [12] Shestopalov, V. & Sirenko, Y. [1989]. *Dynamical Theory of Gratings*, Naukova, Dumka, Kiev.
- [13] Shestopalov, V. & Yatsyk, V. [1997]. Spectral theory of a dielectric layer and the Morse critical points of dispersion equations, *Ukrainian J. of Physics* 42(7): 861–869.
- [14] Shestopalov, Y. & Yatsyk, V. [2007]. Resonance scattering of electromagnetic waves by a Kerr nonlinear dielectric layer, *Radiotekhnika i Elektronika (J. of Communications Technology and Electronics)* 52(11): 1285–1300.
- [15] Shestopalov, Y. & Yatsyk, V. [2010]. Diffraction of electromagnetic waves by a layer filled with a Kerr-type nonlinear medium, *J. of Nonlinear Math. Physics* 17(3): 311–335.
- [16] Sirenko, Y., Shestopalov, V. & Yatsyk, V. [1985]. Elements of the spectral theory of gratings, *Preprint 266*, IRE NAS Ukraine, Kharkov.
- [17] Sirenko, Y. & Ström, S. (eds) [2010]. *Modern Theory of Gratings. Resonant Scattering: Analysis Techniques and Phenomena*, Springer-Verlag, New York. Springer Series in Optical Sciences, Vol. 153.
- [18] Sirenko, Y., Ström, S. & Yashina, N. [2007]. *Modeling and Analysis of Transient Processes in Open Resonant Structures. New Methods and Techniques.*, Springer-Verlag, New York.
- [19] Smirnov, Y., Schürmann, H. & Shestopalov, Y. [2005]. Propagation of TE-waves in cylindrical nonlinear dielectric waveguides, *Physical Review E* 71: 0166141–10.
- [20] Sukhorukov, A. P. [1988]. *Nonlinear wave interactions in optics and radio physics*, Nauka, Moskva. (In Russian).
- [21] Vainstein, L. [1988]. *Electromagnetic Waves*, Radio i Svyas, Moscow. In Russian.
- [22] Vinogradova, M., Rudenko, O. & Sukhorukov, A. [1990]. *Wave Theory*, Nauka, Moscow.
- [23] Yatsyk, V. [2000]. A constructive approach to construction of local equations of irregular dispersion and evolution of fields in a quasi-homogeneous electrodynamic structure, *Usp. Sovr. Radioelektroniki* 10: 27–44. Translated in: *Telecommunications and Radio Engineering*, 56(8&9): 89-113, 2001.
- [24] Yatsyk, V. [2006]. Diffraction by a layer and layered structure with positive and negative susceptibilities of Kerr-nonlinear media, *Usp. Sovr. Radioelektroniki* 8: 68–80.
- [25] Yatsyk, V. [2007]. About a problem of diffraction on transverse non-homogeneous dielectric layer of Kerr-like nonlinearity, *Int. J. Electromagnetic Waves and Electronic Systems* 12(1): 59–69.